ACTIONABLE STITCHED IMAGES FROM AN UNMANNED AERIAL SYSTEM

THESIS

Mr. Brian R. Allen, P.E., USAF

AFIT-ENV-MS-17-M-168

DEPARTMENT OF THE AIR FORCE
AIR UNIVERSITY

AIR FORCE INSTITUTE OF TECHNOLOGY

Wright-Patterson Air Force Base, Ohio

The views expressed in this thesis are those of the author and do not reflect the official policy or position of the United States Air Force, Department of Defense, or the United States Government.

AFIT-ENV-MS-17-M-168

ACTIONABLE STITCHED IMAGES FROM AN UNMANNED AERIAL SYSTEM

THESIS

Presented to the Faculty

Department of Systems Engineering and Management

Graduate School of Engineering and Management

Air Force Institute of Technology

Air University

Air Education and Training Command

In Partial Fulfillment of the Requirements for the

Degree of Master of Science in Engineering Management

Brian R. Allen, P.E., BS

GS-12, USAF

March 2017

AFIT-ENV-MS-17-M-168

ACTIONABLE STITCHED IMAGES FROM AN UNMANNED AERIAL SYSTEM

Brian R. Allen, P.E., BS

GS-12, USAF

Committee Membership:

John M. Colombi, Ph.D.
Chair

David R. Jacques, Ph.D.
Member

Alfred E. Thal, Jr., Ph.D.
Member

Abstract

This thesis investigates the capability of a commercial off the shelf (COTS) unmanned aerial system to accurately capture and represent a portion of an airfield for condition evaluation. Three separate flight tests were performed exploring different means of camera shutter control and altitudes. The individual images captured were then stitched into a single orthomosaic which provides an aerial view that can be used to determine dimensional measurements, geolocation, elevation modeling and situational awareness.

The results found show that COTS hardware and software is possible of capturing images with ground resolution of less than 6 mm. The orthomosaic that was generated proved to maintain dimensional accuracy. The digital elevation model that was generated was able to show terrain elevation differences of less than one foot. This provides a proof of concept that for less than five thousand dollars a civil engineer squadron could have an organic ability to accurately assess and quantify an airbase digitally. This will help ensure that limited resources get to the right place at the right time.

This thesis is dedicated to my colleagues, friends, and family that have provided mentorship, support, and patience throughout my career. Most especially:

To my parents and brother – for being my foundation.

To Megan, Gray, and Devon – for your love and understanding while these thesis pages crawled together. I am looking forward to starting our next chapter together.

Acknowledgments

This research would not have been possible without a substantial amount of help. I would like to start with Dr. John Colombi for taking me on board and assisting with putting my scattered vision into some semblance of order. Dr. Colombi and Dr. David Jacques have taught me all I know about UAVs and flight testing. It was a great experience and one of my highlights at AFIT. Rick Patton, Jeremy Gray, Ben Fain, and Chua also provided great support and assistance. Jeremy has proven to be an exceptional golf cart operator even without GPS.

My sincere thanks to Brian Skibba at AFCEC for sharing his knowledge and experience in airfields. Mike Ambrose at RAF Lakenheath has been a valuable pavement resource since 2011 and I appreciate the consistent support. Thanks to Tracy Meeks for getting me started and the constant support throughout.

Brian R. Allen

Table of Contents

Page

List of Figures

Page

List of Tables

Page

ACTIONABLE STITCHED IMAGES FROM AN UNMANNED AERIAL SYSTEM

I. Introduction

"Use a picture. It's worth a thousand words." – Tess Flanders

Chapter Overview

This chapter will discuss the focus of this research effort and how it was developed. The background and research objectives will be defined. An overview of methods used will provide some insight as to the steps taken. The ending of the chapter provides a preview of the following chapters.

Background

Rarely do leaders have all of the required information at hand prior to having to make decisions (Nex & Remondino, 2014). Which areas of pavement are the worst on the airfield? The runway is 150’ wide x 6500’ long; with limited funding, which concrete slabs need to be replaced this year to maintain operations? Providing an overhead orthomosaic of the area in question from the last few hours with the ability to zoom and measure would be a considerable improvement to the way things are done currently. In this research an orthomosaic will follow the Greenwood (2015) definition of a single image made of overlapping aerial images that have been corrected geometrically to provide a uniform scale and are stitched together.

The USAF Civil Engineer (CE) presently captures the airfield pavement condition by using visual surveys every five years to determine a numerical rating from 0

to 100. The ratings, which represent the Pavement Condition Index (PCI), are categorized as 71-100: Good (colored green), 56-70: Fair (colored yellow), and 0-55: Poor (colored red). PCIs are primarily accomplished by base CE personnel or contractor and interpretations can vary substantially resulting in a non-standardized product that sits in three ring binders or on a few compact discs.

The Chief Scientist of the United States Air Force points to new potential in *Autonomous Horizons* (Endsley, 2015):

> Autonomous systems provide a considerable opportunity to enhance future Air Force operations by potentially reducing unnecessary manning costs, increasing the range of operations, enhancing capabilities, providing new approaches to air power, reducing the time required for critical operations, and providing increased levels of operational reliability, persistence and resilience.

Figure 1 provides an example of the contrast between the final graphic product of a PCI and that of a stitched overhead mosaic. If instant recognition of location of the airfield is not clear, GPS coordinates are available from the orthomosaic.

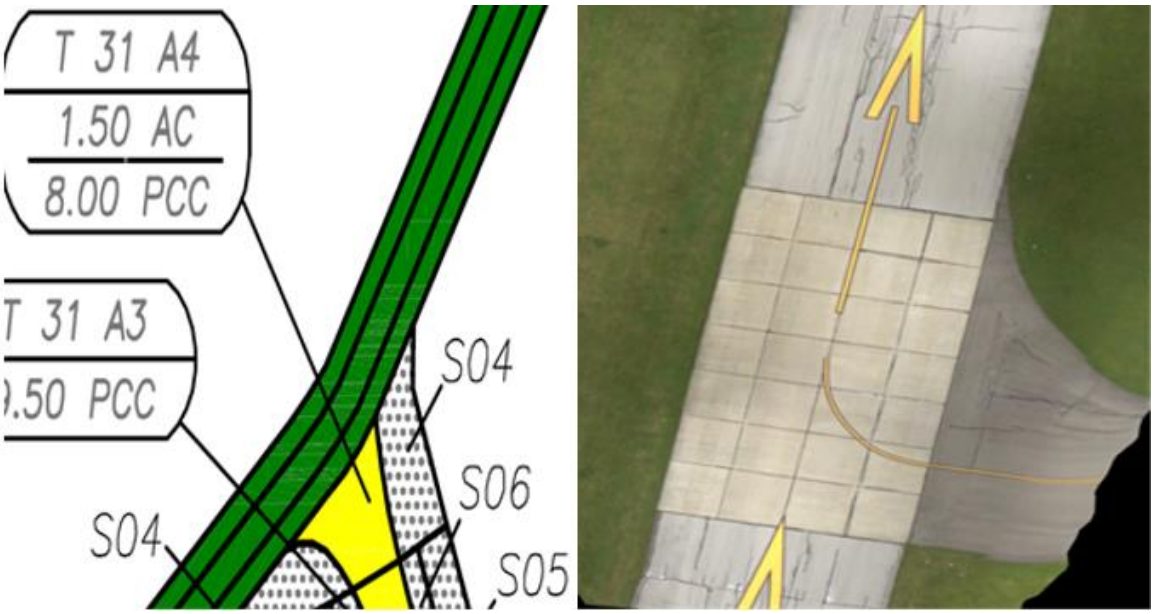

Figure 1: 2016 PCI Section from RAF Lakenheath, UK (left) and, 2016 Orthomosaic Example from Camp Atterbury, IN (right)

While the images in Figure 1 reference two different airfields, the intent is to show the end product produced by the methods currently used and those proposed in this research. The Director of Civil Engineers, Major General Green (2016) highlights the need for a new solution for asset visibility in the *USAF Civil Engineer Flight Plan*:

> The Air Force now needs a capable, competent and technologically-ready force more than ever. Air Force Civil Engineers must look for innovative ways to provide ready forces prepared to deliver required capabilities as the Air Force continues to modernize and recapitalize its installations.

Providing a high quality georeferenced image of an area of interest to a CE commander would be a valuable asset when determining where and when to apply limited resources. With limited resources, one needs to know which square foot of airfield pavement to invest in now. Studies show that investing a small amount at a critical point can save a large repair/replacement down the road (Grandsaert, 2015).

Problem Statement

Runway lengths within the armed forces range from 5,000 to over 13,000 feet with widths from 75 to 300 feet (DoD, 2008). This means an installation can be responsible for up to 3.9 million square feet of pavement for just one runway. This does not include the miles of taxiways and aprons which all make up a functional airfield.

What is the best way to capture, analyze, present, and reference an assessment of an airfield's pavement condition? There has been little change over the past 50 years in the way the USAF has performed this important function. This research will explore the option of using a UAS to capture pavement condition and additional uses a UAS can have at an installation.

Research Objective and Investigative Questions

This research sets out to illustrate that a current commercial off the shelf (COTS) Unmanned Aerial System (UAS) is fit for service and can provide a significant improvement to the way an airfield condition is documented. An airfield is of no use to the mission if the airfield is not operational. Being able to communicate an airfield's current condition is vital to be able to compete for limited sustainment funds or to capture damage sustained from an attack. This research asks the following investigative questions:

1. How can imagery from a COTS UAS be beneficial to a civil engineer squadron?
2. What flight and processing methods provide the best orthomosaic resolution and accuracy?

To quantify the differences in products between different configurations the following values were found for each final product: ground resolution (mm/pixel), dimensional accuracy (X,Y,Z error in mm).

Methodology Overview

The UAS in this project was made up of three parts: the Unmanned Aerial Vehicle (UAV), payload, and ground control station. The collected aerial images were then post processed into both an orthomosaic and digital elevation model (DEM). DEMs provide a digital representation of the terrain by assigning colors to different heights commonly used by geologists, hydrologists, civil and mining engineers (Sulebak, 2000). This section will provide an introduction into the steps taken.

The UAV selected was chosen from the best available airframe and camera from the assets at the Air Force Institute of Technology (AFIT) in 2016. With both multi-rotor and small fixed wing UAVs available, the decision was to select a fixed wing as it provided more range which would be a key consideration when surveying an airfield. The electronic Sig Rascal 110 was settled upon as it is a proven hobbyist aircraft with minimal vibration from its electric motor (Clement et al., 2009).

The payload carried by the UAV consisted of a digital camera, GPS, and intervalometer. A camera mount had been previously installed on the underside of the aircraft near the center of gravity. The Canon SL1 was recently purchased for another project and is utilized commercially for agriculture surveys due to it being one of the smallest digital single-lens reflex (DSLR) frames available. The website *Imaging Resource* notes that it is "the smallest and lightest DSLR that we've ever reviewed."

Pairing it with a short barrel pancake lens maximizes ground clearance within the Sig's landing gear. The 24mm focal length was selected over the 40mm as it provided a larger field of view.

One piece of hardware that was not readily available was a means to control the camera shutter via the autopilot. The autopilot has 14 output ports in a 3 pin configuration, while the camera has a 2.5 mm jack to receive input from a remote control. A cable could be made to connect the two but the autopilot produces signals at 3.3 volts and the camera remote control port expects only continuity between two points of a 2.5mm headphone plug to activate the shutter. A $0.35 optocoupler provided the means to isolate the autopilot signal electronically from the camera. The optocoupler transmits the signal by light which physically isolates the autopilot and camera while still allowing communication. Ground testing was then performed to ensure the connection allowed for camera shutter operation at waypoints by the autopilot.

The ground control station (GCS) consisted of a laptop running Mission Planner and a modem for communication with the UAV. The UAV is semi-autonomous as it handles all navigation except for take-off and landing which are the responsibility of the safety pilot (Meier, Tanskanen, Fraundorfer, & Pollefeys, 2012). Mission Planner software is used on the ground control station to create the flight plan and monitor operation. Mission Planner offers an automatic survey feature which takes into account the camera being used and the altitude and speed being flown. With these values and the requested image overlap and sidelap, Mission Planner will generate the waypoints required to accurately cover the area required. The camera specifics considered include the focal length, sensor size, and shutter delay. The image processing software, Agisoft

Photoscan, provides the overlap and sidelap percentages desired to produce the best composite image. The 80% forward overlap and 60% sidelap referenced ensure that each point is covered more than once. This allows the software to more accurately determine location and provide the most realistic representation in the composite orthomosaic.

Once the flight plan is created, it is then written to the Pixhawk autopilot which resides on the UAV. Communication between the GCS and the UAV is maintained by modems which provide the ability to make adjustments during flight. Once the test pilot has the UAS in the air and is satisfied with how the aircraft is performing in current conditions the test pilot can then switch control of the aircraft from manual to auto. In auto mode, the aircraft is autonomous and will make the appropriate adjustments to progress to the next waypoint. When wind velocity and/or direction changes, the autopilot will compensate to maintain the mission waypoints.

Three scenarios were initially flight tested at Camp Atterbury, IN on 2 May 2016. The first two used the camera collecting images on its own with a intervalometer controlling the shutter and Canon global positioning system (GPS) recording location. The third test relied solely on the Pixhawk autopilot to control shutter and GPS.

A second round of testing was performed at the Wright Patterson Air Force Base (WPAFB) Area B airfield. These tests also incorporated test articles upon suggestion by the Air Force Civil Engineer Center (AFCEC) as they are looking into Airfield Damage Repair (ADR) assessment. Test articles included three sections of pipe: 2” diameter by 4” length, 3” diameter by 8” length, 8” diameter by 20” length. A crater was replicated with a tarp and three 50-pound bags of sand. This combination produced a circular 2”

mound that was 96” in diameter. A one-gallon bottle of water was punctured prior to launch to get a representative spill size.

After reviewing images captured during the second flight test the ground resolution of the test articles was found to be inadequate. Both of the first two flight tests were at an altitude of 60 meters. Based upon these findings, it was determined that the third test should be at the minimum altitude allowed by the current memorandum of agreement which is 32 meters. The test articles for the third test included the three pipe sections and a yard stick. The yard stick was included as it was a standard dimension that is relatable to most while the pipe sections are not standardized.

Preview

The following chapters will further detail the capabilities presently available from COTS products and the images that were obtained and processed. Chapter II summarizes the literature reviewed regarding UAS applications, configurations, and orthomosaic generation. Chapter III describes the methodology used in the research. The following will be described: test procedures, image analysis, prefiltering, and orthomosaic generation. Chapter IV presents the flight test results, the orthomosaics generated, and compares test article measurement accuracy. Chapter V will provide conclusions, answers to the original research questions, and suggestions for further research.

II. Literature Review

Chapter Overview

This chapter explores the central topics of unmanned aerial vehicle (UAV) imagery based on existing studies and possible applications to USAF Civil Engineering (CE). The primary CE application researched in this paper is airfield pavement assessment and will be covered first. Other applications of UAV imagery are explored to be followed by image processing techniques.

Airfield Pavement Assessment

Air Force Pavement Engineering Assessment Standards

The Air Force Pavement Evaluation Program is defined in Air Force Instruction 32-1041 which was updated on 10 September 2013 and supersedes the 1994 version. One of the program elements is to perform Pavement Condition Index (PCI) surveys for airfield and road networks. The PCI works to identify and capture pavement condition as vehicle traffic and the environment will degrade and distress the pavement over time. PCI surveys are to be performed on a 5-year cycle for main operating bases and auxiliary fields. The PCI represents a 0 to 100 rating based on a visual pavement survey and provides the Air Force a metric to compare maintenance and repair project needs across the full AF airfield inventory. The PCI rating scales are shown in Figure 2 and show how the number of scales have been reduced or simplified. There will be variability associated with an individual's definition of a Very Poor or Serious piece of pavement and the numeric value assigned. This variability is a problem when one project is funded

over another based on a PCI being a few points lower. The definitions listed in Table 1 attempt to increase consistency among raters, but there is still potential for improvement in the way pavement condition is captured, presented, and stored.

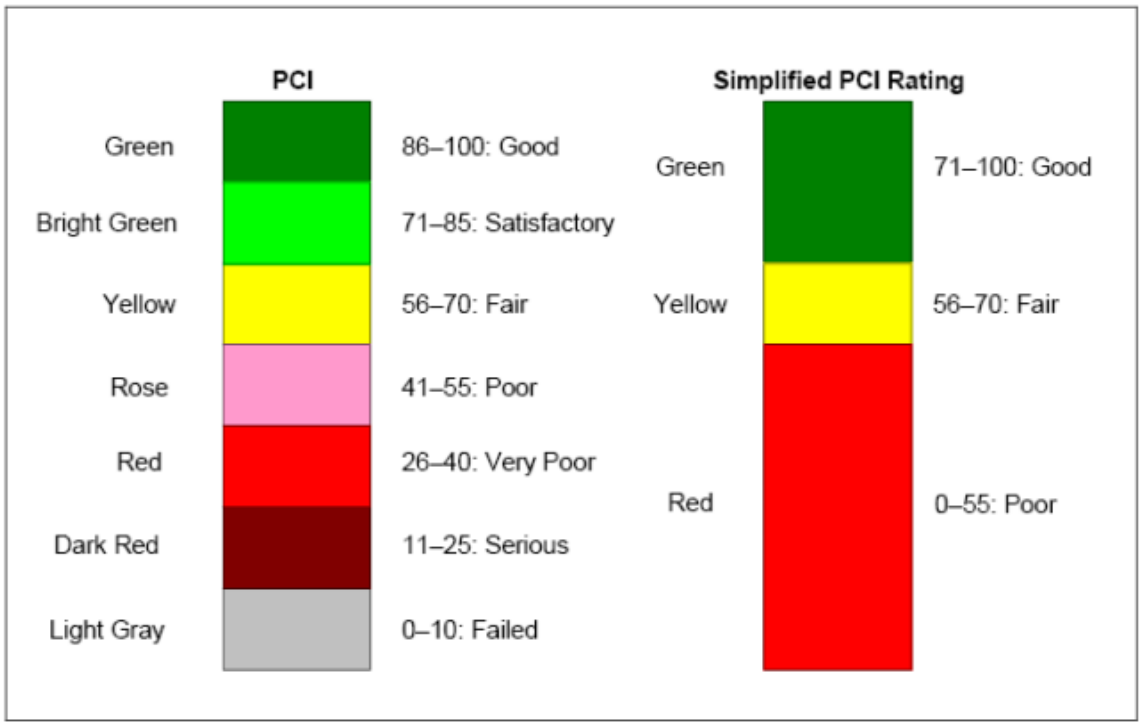

Figure 2: PCI and Simplified PCI Rating Scales (AFI32-1041, 2013)

Table 1: Definition of PCI Ratings (AFI32-1041, 2013)

Rating	Definition
86–100	GOOD: Pavement has minor or no distresses and should require only routine maintenance.
71–85	SATISFACTORY: Pavement has scattered low-severity distresses that should require only routine maintenance.
56–70	FAIR: Pavement has a significant amount of generally low- and medium-severity distresses. Near-term M&R needs may range from routine to major.
41–55	POOR: Pavement has low-, medium-, and high-severity distresses that probably cause some operational problems. Near-term M&R needs may range from routine up to a requirement for reconstruction.
26–40	VERY POOR: Pavement has predominantly medium- and high-severity distresses that cause considerable maintenance and operational problems. Near-term M&R needs will be intensive in nature.
11–25	SERIOUS: Pavement has mainly high-severity distresses that may cause operational restrictions; immediate major repairs are needed.
0–10	FAILED: Pavement deterioration has progressed to the point that safe aircraft operations may no longer be possible; complete reconstruction is required.

CE Related UAS Research

Researchers in the past two AFIT graduating classes have had researchers who explored autonomous vehicles and their applications within the USAF Civil Engineering community. Both focused on asset management through condition assessments using images captured by autonomous vehicles. Grandsaert (2015) focused on pavement crack detection from above, while Meeks (2016) focused on pipe crack detection below ground. Both studies utilized autonomous vehicles to collect images which were then post processed to automatically identify and quantify cracks. The algorithm findings were then compared to those of a subject matter expert viewing the same images with 36% efficiency.

A group from the United States Air Force Academy looked into ways to reduce the time required to return an airfield to operational status after an attack (Anderson, Pasque, Lane, Pond, 2017). By using semi-autonomous systems, they were able to

reduce the time to assess a runway from 2 hours to 25 minutes without putting humans in danger. The visual product provides more information regarding scale, location, and variation. "The system provides a unique capability not yet realized by the United States Air Force and has the potential for farther reaching applications."

Figure 3 shows some of the challenges of integrating detailed images of areas of interest onto a runway. The satellite image below is of a portion of the 2,000 ft by 75 ft runway at the U.S. Air Force Academy. Eight individual pictures were taken by a UAV.

Figure 3: Runway Analysis Overlaid on Satellite Image (Anderson, Pasque, Lane, Pond, 2017)

Timely pavement maintenance is a sound investment. Schenbele et al (2015) note that the cost of reconstruction can be more than three times higher for deteriorated roads that did not receive proper maintenance. The authors also noted that transportation engineers often do not know the capabilities of UAVs which has led to limited integration into assessments.

Inspection

Construction safety management has not adopted new technology as much as it should (Irizarry & Walker, 2012). One way to ensure and promote construction safety is through frequent and direct observation. Irizarry and Walker suggest that UAVs should be used as an observation tool to provide real time video and communication capabilities.

UAVs can provide better images of critical civil infrastructure bridges, towers, power plants, etc., at a lower cost while improving personnel safety (Morgenthal & Hallermann, 2014). Damage detection of roof and building surfaces allows one to plan for repair based on the remotely captured images or videos.

The Smithsonian National Air and Space Museum recently added the ScanEagle N202SE to its collection (McIntosh, 2016). This UAV performed the first ever commercial beyond the line of sight inspection in 2013. Its mission was to collect data for forecasting ice floe off the northern Alaskan coast. In 2015, the UAV became the first in the contiguous United States to operate commercially beyond the line of sight inspecting 140 miles of railroad track in New Mexico.

The Intel Corporation used 300 UAVs to provide a dynamic light show behind Lady Gaga at the Super Bowl 41 halftime show (Gendreau & Levin, 2017). Nonentertainment applications referenced in Gendreau and Levin's (2017) article include insurance documentation of property damage, precision agriculture, and osprey nest inspection. ABC news divisions now have a UAV to cover breaking news, claiming that UAVs would "change the way we told stories forever" (Gendreau & Levin, 2017).

San Diego Gas & Electric uses UAS to locate power outage causes, gas and power line inspection, remote area infrastructure assessment, emergency management,

and to minimize noise pollution instead of having to use helicopters (San Diego Gas & Electric, n.d.).

Mappping

Barry and Coakley (2013) found that aerial imagery provided 1:200 map scale accuracy and predicted that UAV photogrammetry will replace topographical surveying data collection in the future. They utilized Agisoft Photoscan to produce a orthomosaic and digital elevation model which was then imported into ArcGIS. ArcGIS is one of the industry leaders in geographic information systems and allows for data to be collected and represented graphically.

Photoscan allows for several different means of exporting the orthomosaic including KMZ, which zips all of the image information into a format that Google Earth can open directly. Google Earth will provide satellite imagery of the surrounding area that was not captured by the UAV. Google Earth also allows for the measurement and comparison of an area over time with satellite images dating back to 1994.

Disaster Support

The ability to respond to a humanitarian disaster appropriately and quickly is paramount to saving as many lives as possible (Tatham, 2009). Performing a needs assessment to understand the scale and resources required is the first step, and there are applications when a UAV would be the best tool available. Consider the assistance a UAV can provide to the transition, recovery, and prevention phases of disaster relief.

Agriculture Applications

One of the most currently used commercial applications for aerial imagery captured by a UAV is in agriculture. For decades, farmers have used manned aerial

vehicles to inspect and treat their fields. With fields that span hundreds of acres, environmental conditions can vary significantly. The visible crop condition on the accessible perimeter does not accurately represent those throughout. Moisture levels can vary significantly based on elevation, shade, wind, etc. Pests do not necessarily affect the whole field and different pests can be in different areas. Being able to identify, measure, and communicate the application plan with an image is of high value to a farmer. Crop yields are increased when the right treatment is applied to the right area at the right time (Swain et al, 2010). Measuring crop growth rate is a key metric in crop development and increasing ground resolution led to a more acurate surface model (Holman et al, 2016).

Conservation

UAVs provide a low-cost remote sensing technology to capture changes in species location and forest foliage (Koh & Wich, 2012). One other benefit of a UAV is that it provides more control to be able to capture images when the conditions are clear. With cloud cover a consistent problem in the tropics, satellite images can be unreliable. The ability to consistently capture images at a lower cost provides the ability to track the numerous land use changes. Dr. Rose highlighted the UAV as a best approach to provide high resolution images that can allow a more detailed analysis of change in an area (Wildlife Conservation Society, 2014). Remote sensing that provides high resolution information is an advancing tool in forest modelling (Wallace et al, 2016).

Image Processing

Orthomosaic Software

An orthomosaic image is one that is generated by orienting and merging multiple overlapping images into one mosaic; it is also referred to as stitching. Gross (2015) compared three of the most common software packages currently available: Microsoft Image Composite Editor, Pix4D Pro Mapper, and Agisoft Photoscan. Both Photoscan and Pro Mapper are based upon the structure from motion (SfM) algorithm, which utilizes well defined geometric features from different images at different angles to build a point cloud (Wallace et al, 2016). There was no documentation available on the algorithm(s) used by Microsoft Research in Image Composite Editor.

Table 2: Software Comparison (Gross, 2015)

	Geometric accuracy	Visual quality	Cost	Ease of use
ICE	2	1	1	2
Photoscan Pro	1	3	2	1
Pix4D	1	2	3	3

The images collected in Gross's research were of the Braeburn Marsh Preserve, which contains reed canary grass, wet-mesic prairie, typha marsh, and wood vegetation; these are not typically found on an airfield. Gross concluded that each software package was better than others in terms of geometric accuracy, visual quality, cost, and ease of use.

Light Detection and Ranging (LIDAR)

Another tool used to gather modeling information is a light detection and ranging (LIDAR) sensor (Jensen & Matthews, 2016). With the desired output of this research to be a composite image LIDAR was not further considered. Research shows that point clouds from UAS aerial images are replacing or augmenting LIDAR applications (Jensen & Matthews, 2016).

Digital Elevation Models

One product generated by Photoscan is a digital elevation model (DEM), which represents the image terrain with varying shades of color per pixel to represent different elevations. Greenwood (2015) relates them to a topographical map that allows one to see the underlying surface. The Michigan Department of Transportation has used digital elevation models of bridges to generate a spall value used to compare bridge conditions (MTU, 2015).

Including Vehicle Position to Minimize Error

The Canon GPS writes latitude, longitude, and altitude details into each image file as it is captured. This information allows the orthomosaic software to build a map of the camera positions which aids in stitching. Including the UAV pitch and roll details was shown to reduce error by 93.3% (Xiang & Tian, 2011).

Digital Image Processing

Histogram equalization distributes the intensity values of an image more evenly across the range. Locally adaptive histogram equalization applies different functions in different regions depending on the characteristics in that region (Szeliski, 2010). Grandsaert (2015) used the technique for both lighting and image intensity levels.

Summary

This chapter provides the background on the current USAF airfield pavement assessment program which has remained largely unchanged over the past fifty years. The utilization of UAVs to capture images for decision making was discussed. Finally, some of the different ways to enhance individual still images were explored.

III. Methodology

Chapter Overview

This chapter outlines the ways the investigative questions of orthomosaic resolution were addressed. The research method is divided into three aspects. First, a review of the materials and equipment used to collect the images. Second, the flight testing scenarios are described. Finally, the image processing of stitching images into an orthomosaic is discussed to include the software and options selected.

Materials and Equipment

The materials and equipment used for this research included a UAV, camera, ground control station, communication, and image processing software. Detail will be provided as to the selection process, installation, settings used, and operation.

Unmanned Air Vehicles

The aircraft selection for this research focused on the nearly 20 different assets currently available at AFIT. The two main categories of unmanned aerial vehicles are multirotor and fixed wing (Tahar & Ahmad, 2013). Multirotors provide better control, payload stability, and more flexibility for take-off and landings. The negatives to a multirotor are the limited range within a battery charge and the lack of options if there is a loss of electrical power. A fixed wing aerial vehicle provides the most range, thus allowing it to cover the most area. The fixed wing vehicle's ability to glide also allows for the possibility of minimizing impact if there is a loss of motor power. The downside

to a fixed wing is control, payload stability, and requiring an area/equipment to take-off and land.

The UAV chosen for this research was the 110" wingspan electric Sig Rascal shown in Figure 4. The model had an electric motor which produces less vibration to affect the payload, as opposed to the gas motor model shown in Figure 4. The manufacturer refers to this model as a "versatile workhorse" that is being used by universities and government agencies for capturing aerial pictures and video.

Figure 4: Sig Rascal 110 (SIGPlanes, n.d.)

Autopilot

Control of the Sig Rascal once in the air was provided by a Pixhawk autopilot, shown in Figure 5, which is one of the leaders in UAV flight controllers. The Pixhawk receives the waypoints from the ground control station and works to position the UAV to meet those points. Vehicle control is done by the autopilot adjusting the throttle, ailerons, elevator, and rudder. The UAV's response to those signals are verified through the GPS.

Figure 5: Pixhawk Autopilot (3D Robotics, n.d.)

Ground Control Station

The Ground Control Station (GCS) consisted of a laptop, modem, and radio. The modem and radio allowed for communication between the aircraft and safety pilot respectively. The engine in the GCS is the Mission Planner software which is a free and open source application that is able to run on a standard laptop. Mission Planner provides a means for the operator to communicate the mission to the UAV for execution. The operator defines the survey area by clicking on points on a map within Mission Planner to define the survey area perimeter with a polygon. In Figure 6 the survey polygon was defined with only four points represented visually with the red pins and red connecting lines. The polygon shape is flexible and multiple points are possible for areas that are not linear. Once the operator has provided the survey area border MP will then generate the required waypoints to ensure that the UAV covers the area in a manner that the camera will provide adequate image representation.

With the UAV on the ground, the laptop is connected directly to the UAV with a standard USB cable but once the UAV is in the air cable length can be an issue. A

wireless solution is provided through telemetry modems. One modem is connected to the ground control station laptop and the other is connected to the UAV Pixhawk autopilot.

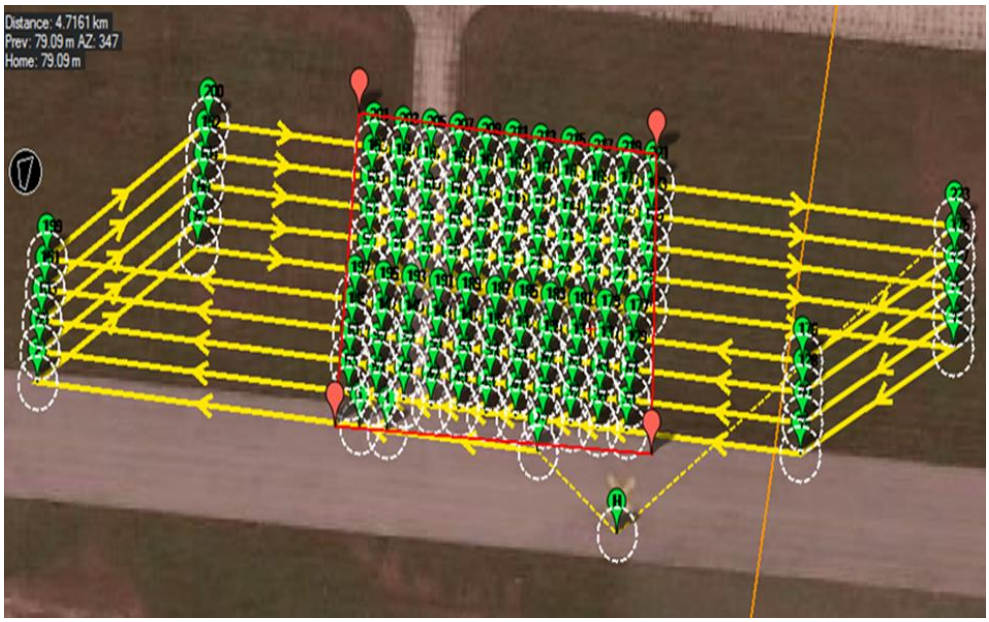

Figure 6: Mission Planner Survey Area Test #3

Camera System

The camera body selected was the Canon SL1 illustrated in Figure 7. The SL1 is one of the smallest and lightest DLSR cameras available. Both metrics are important when mounting to a UAV. The 24mm pancake lens was used as it provided both the best combination of ground clearance and field of view. The Canon GP-E2 GPS receiver was utilized as it writes altitude, latitude, and longitude directly to each image file. Figure 8 shows the receiver in its typical mounting position on the top of the camera in the "hot shoe" circled in red.

Figure 7: Canon SL1 with pancake lens (Canon, n.d.)

Figure 8: Canon GP-E2 GPS Receiver (Canon, n.d.)

The camera shutter was controlled by both a cable from the Pixhawk autopilot and an intervalometer. Both plug into the 2.5 mm remote jack in the camera body and complete the circuit between the camera shutter and ground electrically. The Pixhawk sends a signal when the UAV reached the prescribed waypoint. The intervalometer is based upon time alone with options including time between shots, the length of time the shutter is opended, delay between shots, and total shots possible. Figure 9 shows an intervalometer similar to the one used for the research.

Figure 9: Intervalometer (Neewer, n.d.)

Software

The two software packages used were Agisoft Photoscan and Google Earth. Photoscan was used to generate the orthomosaic image and digital elevation model, while Google Earth was used to view the orthomosaic image. Google Earth also allowed for the ability to measure and locate items within the orthoimage.

Cost

Table 3 lists the approximate costs one should expect to pay to purchase the items used in this research. The significant difference in price difference for Agisoft Photoscan is due to two editions, standard and professional, being available in both educational and professional versions. The various additional items one would need to operate a UAV such as radio, batteries, charger, modems, etc., are not listed nor is a laptop.

Table 3: Equipment Used

Type	Model	Cost
UAV	Sig Rascal 110	$1,000
Camera	Canon SL1	$500
Lens	Canon 24mm	$150
GPS	Canon GP-E2	$240
Intervalometer	Neewer EZa-C1	$20
Software	Agisoft Photoscan	$60-3,500
Software	Google Earth	$0

Procedures

Ground Testing

Flight testing is expensive and time consuming regardless of whether the vehicle is manned or unmanned. A UAS takes a team to schedule range time, prep the UAV, charge batteries, transport, have a qualified safety pilot, spotter, etc. Since AFIT has multiple researchers looking to fly for their research; therefore, it is critical to maximize the flight time available.

Ground testing as many scenarios as possible saves time and money; it also minimizes pressure on the researcher during flight tests. For this research, ground testing focused on camera shutter control via the two different methods. The first method was

via the standard intervalometer at a predetermined number of seconds regardless of location. The second method was controlling the camera shutter release at waypoints in the air through Mission Planner and Pixhawk.

Ground testing was performed primarily in the AFIT parking lot. In Mission Planner, a survey area of a portion of the parking lot was developed. The manned ground vehicle used was a golf cart carrying a Pixhawk, laptop, and camera. As the golf cart visited the designated waypoints, the camera shutter was released through the optocoupler cable which connected the camera remote control terminal to the Pixhawk relay pin 54, AUX OUT 5, Relay 13. The signal was passed through Mission Planner when a Do-Digicam-Control command was written after the desired waypoint was reached.

Test Articles

As discussed previously, one of the top challenges faced by the United States Air Force is getting an airfield back into operation as quickly as possible after an attack. One of the first steps is to ensure there is no unexploded ordnance on the airfield and quantify the amount of repair required.

Capturing digital images of the airfield via a UAV allows for easy distribution to experts so they can assess, identify, and plan without putting airmen at risk. Brian Skibba, Chief Airbase Acquisition Branch (CXAE) Air Force Civil Engineer Center, graciously recommended the dimensional values from real-world experience listed in Table 4.

Table 4: Test articles used in Flights 2 and 3

Explosive Devices: (pipe sections)	Explosive Damage: (sand ring)
2" diameter by 3" length	96" diameter, 2" high
3" diameter by 8" length	
8" diameter by 20" length	

The AFIT model shop was able to obtain most of the pipe sections. To replicate explosive damage, a tarp and three 50-pound bags of sand were used to form a ring. This combination produced a circular 2-inch mound, 96 inches in diameter, that was placed in the area of interest. Figure 10 provides ground level images of both types of test articles used.

Figure 10: 3"x8" pipe section left, 96" dirt ring right

Flight Path Generation

Image processing software uses common points in images to locate and merge into the orthomosaic. To ensure the software has the enough common points to perform these functions, a percentage of forward overlap and sidelap is entered into Mission Planner, which it considers when generating the required waypoints to survey the area of

interest completely. The rectangles in Figure 11 indicate the area an image will cover on the ground. The shading is to highlight the difference between successive images.

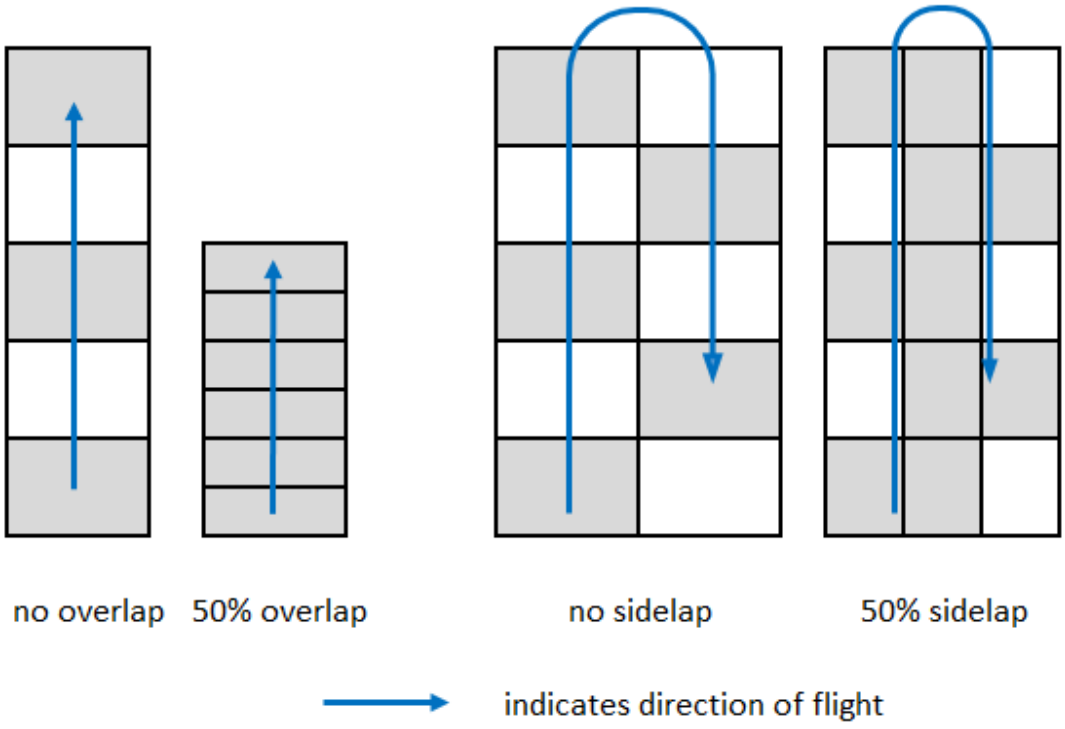

Figure 11: Overlap and sidelap examples

The length and width of the rectangles in Figure 11 are set by the camera field of view and the altitude of flight. The amount of image overlap is dependent on three things: the flight altitude, groundspeed of the aircraft, and time required to capture successive images. The Canon 24 mm lens angles of view are 35º vertical, 50.5º horizontal, and 59.2º diagonal as shown in Figure 12.

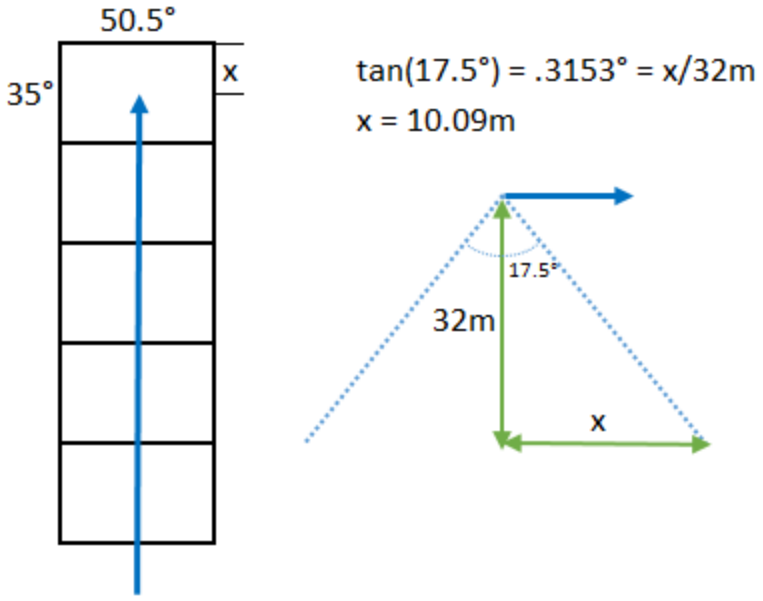

Figure 12: Overlap calculation

Based on the calculation shown in Figure 12, a UAS containing a Canon 24 mm lens at 32 m elevation will capture an image covering a rectangle 20.18 m by 30.18 m. The more critical value is the 20.18 m as that is the direction of travel of the UAV. Photoscan recommends at least 80% of forward overlap for orthomosaic and digital elevation model generation, which proved to be a challenge. The lowest comfortable groundspeed of the Sig Rascal as configured was 17 m/s leaving only a 15% forward overlap if operating the camera shutter at one-second intervals. Operating at a higher elevation would provide a greater coverage area but would decrease resolution.

The minimum time to operate the camera shutter is dependent on two things: (1) the ability of the camera to process one image and be ready to capture the next and (2) the minimum setting of the intervalometer. The website *Imaging Resource* lists the cycle

time of the SL1 for a single shot RAW image at 0.32 second and autofocus lag time at 0.264 second. The intervalometer minimum interval setting is one second. Ground testing confirmed that the SL1 could autofocus capture and store images at the one second interval directed from the intervalometer.

Image Processing

After the flight, there are hundreds of large file size images with no obvious order. On an airfield this is a problem as there are purposefully not many features other than pavement and grass. Figure 13 provides a snapshot of the challenge faced and one of the strengths of an orthomosaic.

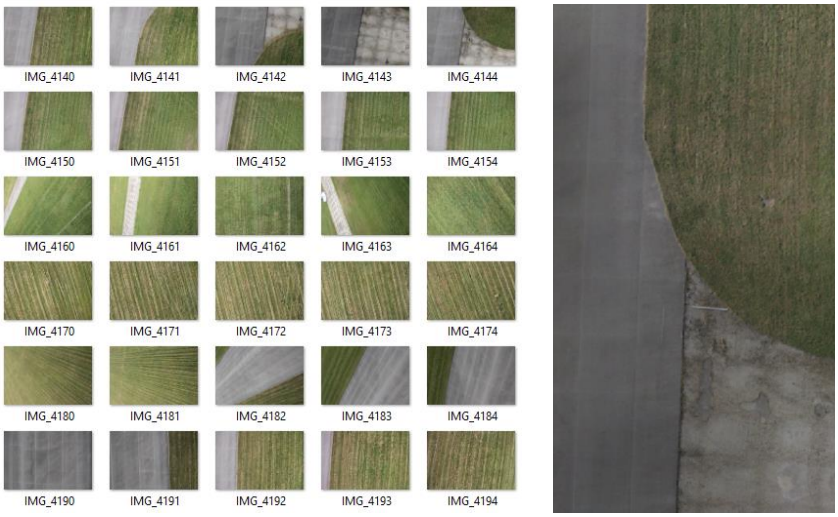

Figure 13: Comparison of Flight 3B image presentation

One of the benefits of the camera saving images in the Canon Raw Version 2 (CR2) format and using the Canon GPS is that details about the camera and GPS information about the picture are written into each image file. These file details are

readily available for view as illustrated in Figure 14. Trying to match images to their location via the Mission Planner TLOG proved to be challenging and time consuming.

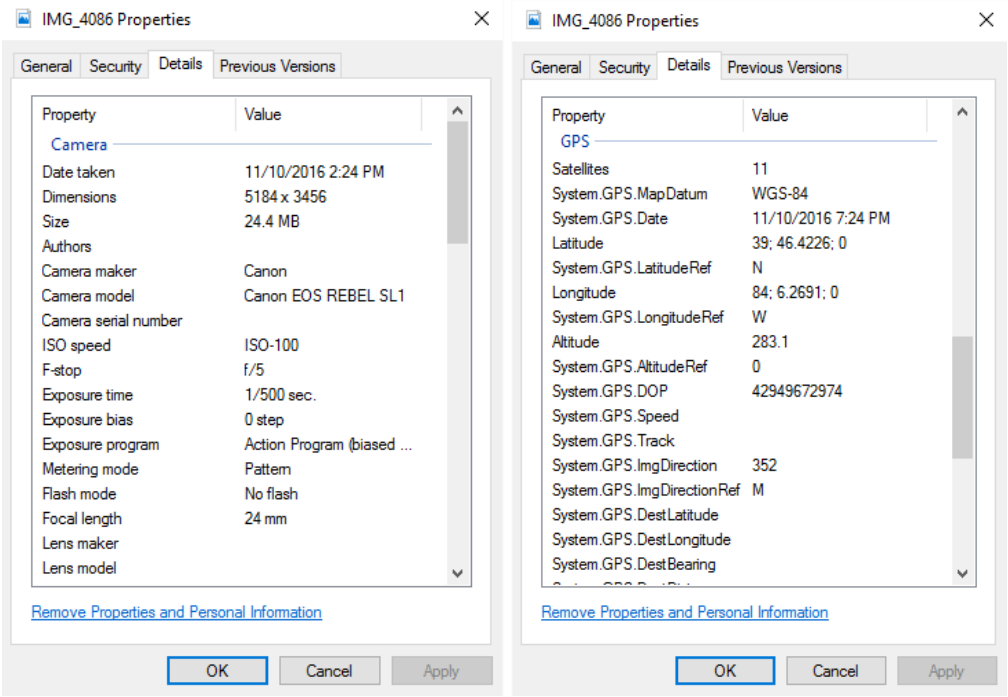

Figure 14: Image file details example via Windows File Explorer

The image file GPS details are used by Photoscan to assemble the camera positions and location from which the image was captured. These positions are represented by small blue spheres in the Photoscan Mode view. Camera calibration information should be verified to ensure focal length and pixel size is accurate within Photoscan. For all of these flights, the values did not change (pixel size: 0.004384 mm, focal length: 24 mm).

Agisoft Photoscan guides the user through the project workflow with an input of multiple aerial images and an output of an orthomosaic and digital elevation model. A diagram of these steps and an example of the output is shown in Figure 15.

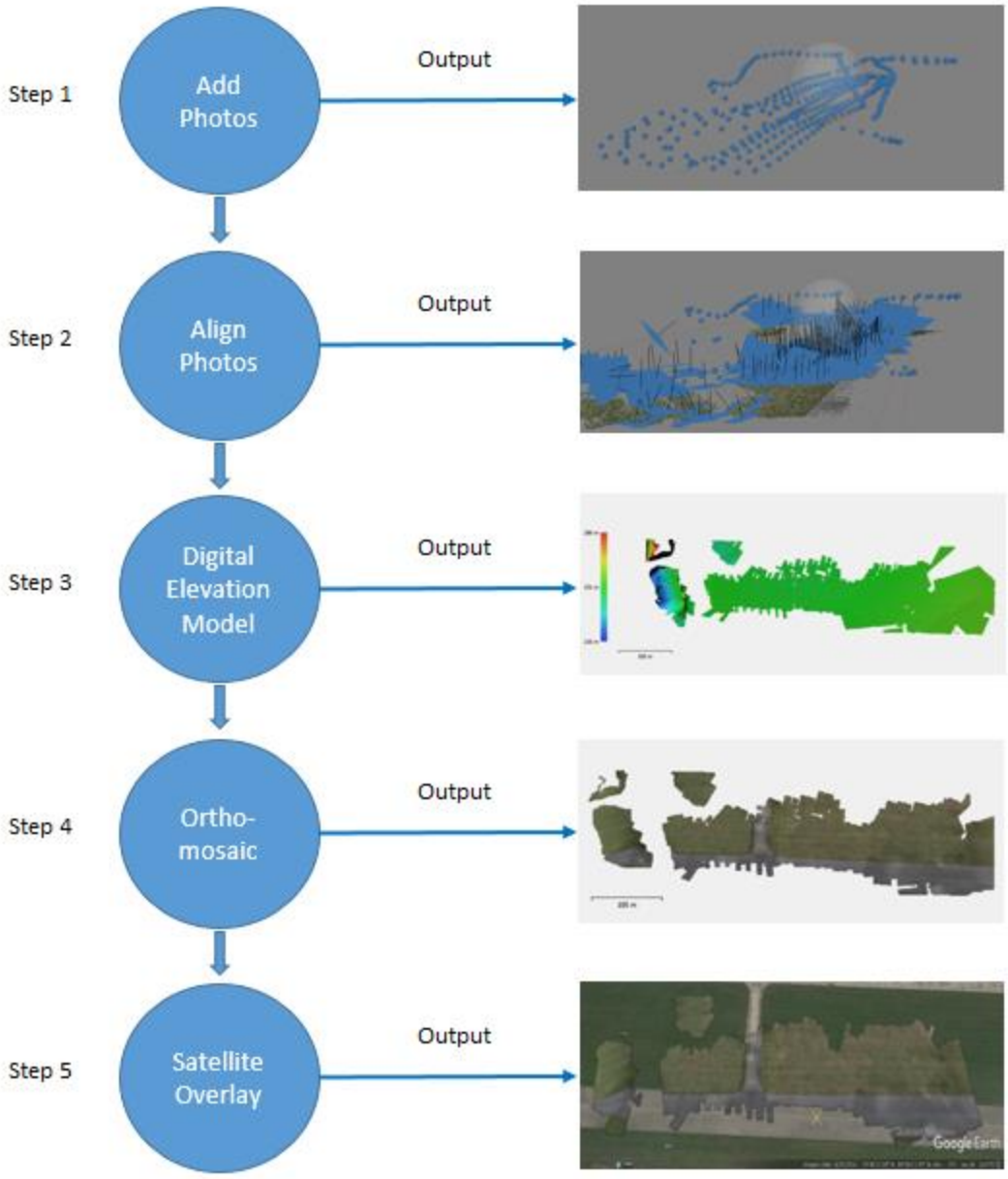

Figure 15: Image Processing Methods and Outputs

Step one is to add the aerial images to be processed. When the intervalometer was used to control the camera shutter, the images captured while on the ground were not included in those to be processed. Photoscan lists nine different image file formats

available for selection which do not include Canon's CR2. Fortunately the CR2 images were able to be used directly by Photoscan after selecting the All Files option without any issues.

Step two is to align the photos in which Photoscan works to match common points and form a sparse point cloud model with the data points being added to one common coordinate system. Photoscan uses the structure from motion algorithm, which utilizes the different angles available on a common feature, to build the point cloud. This highlights the importance of the overlap and sidelap values used when defining the survey area.

Step three is when the software builds a digital elevation model (DEM) by assigning depth information to the 2-dimensional image. Resolution can be maximized and processing time reduced by adjusting a bounding box to focus on the area of interest as shown in Figure 16. Care should be taken to ensure that the red rectangle that forms the base of the bounding box is below the point cloud to ensure all of the image is captured.

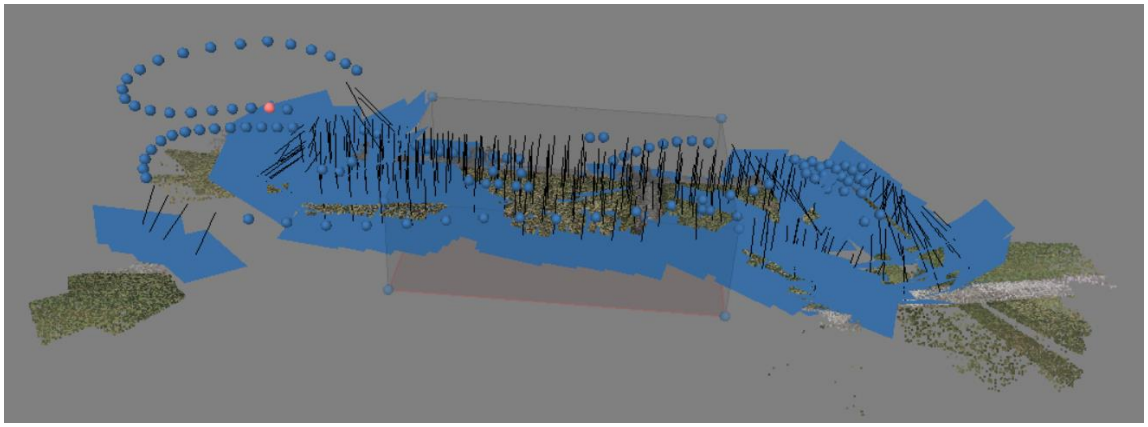

Figure 16: Flight 3B bounding box to focus on area of interest

Step four generates the orthomosaic image of the area included within the bounding box. This image is measurable and location information is provided within Photoscan. A negative within Photoscan is that the orthomosaic is isolated and not relatable to the surrounding area.

Step five is made possible by utilizing the export orthomosaic option within Photoscan to generate a Google KMZ file. This file can then be opened by Google Earth which places the orthomosaic into position on satellite imagery.

Summary

This chapter provides an overview of the material and equipment utilized for this research effort to include the UAS and image processing software used. The procedures taken were also provided as to how the images were gathered and processed to generate an orthomosaic. The results will then be compared and quantified in the following chapter highlighting how the best results were obtained.

IV. Analysis and Results

Chapter Overview

This chapter contains the flight test results, orthomosaics generated, and test article measurement comparisons. Details will be provided regarding the steps taken, time required to process, and resolution obtained. The information provided in this chapter will provide the justification for the interpretation in the following chapter on the research questions.

Results

Flight Test 1

The primary goal of this flight test was to capture images in different ways to be able to compare the GPS output of the Pixhawk autopilot GPS and the Canon GPS. To gather data via the Pixhawk GPS, the camera remote control jack was connected directly to the Pixhawk through the optocoupler cable. When the intervalometer was utilized for control of the camera shutter, it was plugged directly into the remote control terminal of the camera. The details of the three flights on 2 May 2016 at Camp Atterbury, IN, are listed in Table 5.

Table 5: Flight Test 1 Details

Flight	Images	Shutter	GPS
1A	123	Pixhawk	Pixhawk and Canon
1B	244	Intervalometer	Pixhawk and Canon
1C	52	Pixhawk	Pixhawk

Flight Test 2

The primary goal of this flight test was to build on the findings from flight test 1 and to merge the aircraft position at the moment the image was captured with the positional information from the Canon GPS. One of the main findings from the first flight test was that the image locations defined by the Pixhawk GPS and the Canon GPS were nearly identical. The benefit with the Canon GPS was that it wrote the GPS details directly to the image file. This was much easier than trying to find the camera commands within the tlog file written by Mission Planner. The test articles suggested by AFCEC were also introduced on the ground to form an area of interest.

Challenges were encountered with the Pixhawk being unable to control the camera shutter as it had during the first flight test. This led to multiple unsuccessful attempts to rectify the problem in the field. Because of this, both of the flights in which images were collected were done with the intervalometer. Table 5 lists the specifics from those two flights on 13 October 2016 at WPAFB Area B airfield.

Another objective of this test was to improve the ability of the UAV to follow the survey flight pattern. This was addressed in two ways: along the survey route and through UAV handling. The two grid options used in Mission Planner were the Overshoot and Leadin. Overshoot adds an additional waypoint at a prescribed distance past the area of interest to provide the UAV time to make the turn. Leadin creates a point also outside the area of interest for the UAV to target along the next row, thus allowing the UAV to be straight and level upon entry. The Min Lane separation plan option was used to allow for the turning radius of the UAV. The Sig Rascal was also tuned and rudder was added to the turns to improve handling and turn radius. The initial survey

grid generated by Mission Planner is shown in Figure 17, and the modified version is shown in Figure 18. The details of the two flights which captured images on 13 October 2016 at the Area B airfield at WPAFB, OH, were previously listed in Table 5.

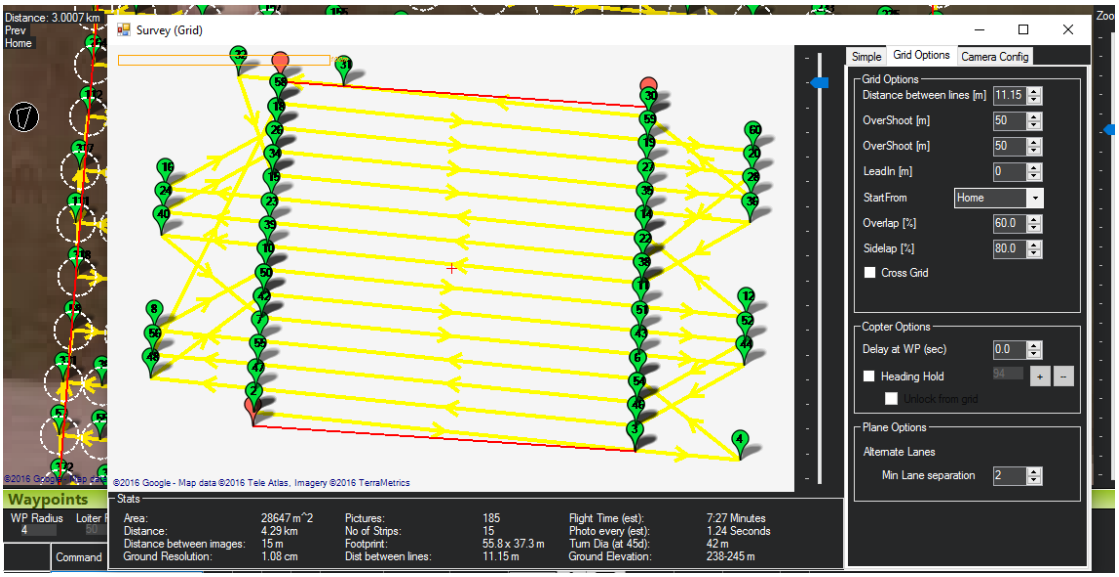

Figure 17: Flight 2 Initial Survey Flight Plan

Figure 18: Flight 2 Adjusted Survey Flight Plan

Table 6: Flight Test 2 Details

Flight	Images	Shutter	GPS
2A	352	Intervalometer	Canon
2B	169	Intervalometer	Canon

Flight Test 3

Efforts were made on the ground to correct the issue with Pixhawk control of the camera shutter release to include updating the Mission Planner software version, different command combinations, and relay pin numbers. The optocoupler was tested on its own and verified to still be functional. In the end none of these attempts were successful in regaining shutter control via the autopilot.

Image resolution viewing the test articles in Flight 2 at 60 meters altitude was unsatisfactory. The decision was made to capture images at the best resolution possible which was at an altitude of 32 meters; this gave a 2-meter cushion from the current Area B UAV hard deck of 30 meters. The camera was also switched from full auto to sport mode to assist with blur. Table 7 provides additional information as to the test settings on 11 November 2016 at the WPAFB Area B airfield.

Table 7: Flight Test 3 Details

Flight	Images	Shutter	GPS
3A	614	Intervalometer	--
3B	401	Intervalometer	Canon

Image Processing

Using the methods previously described, the aerial images were loaded into Photoscan and processed for each flight.

Flight 1A

The Mission Planner survey function needed to be adjusted as the default pattern generated by Mission Planner was not possible for the UAV to follow as shown in Figure 19. The rows were too close together for the aircraft to be able make the turn which resulted in an erratic flight plan as illustrated in Figure 20.

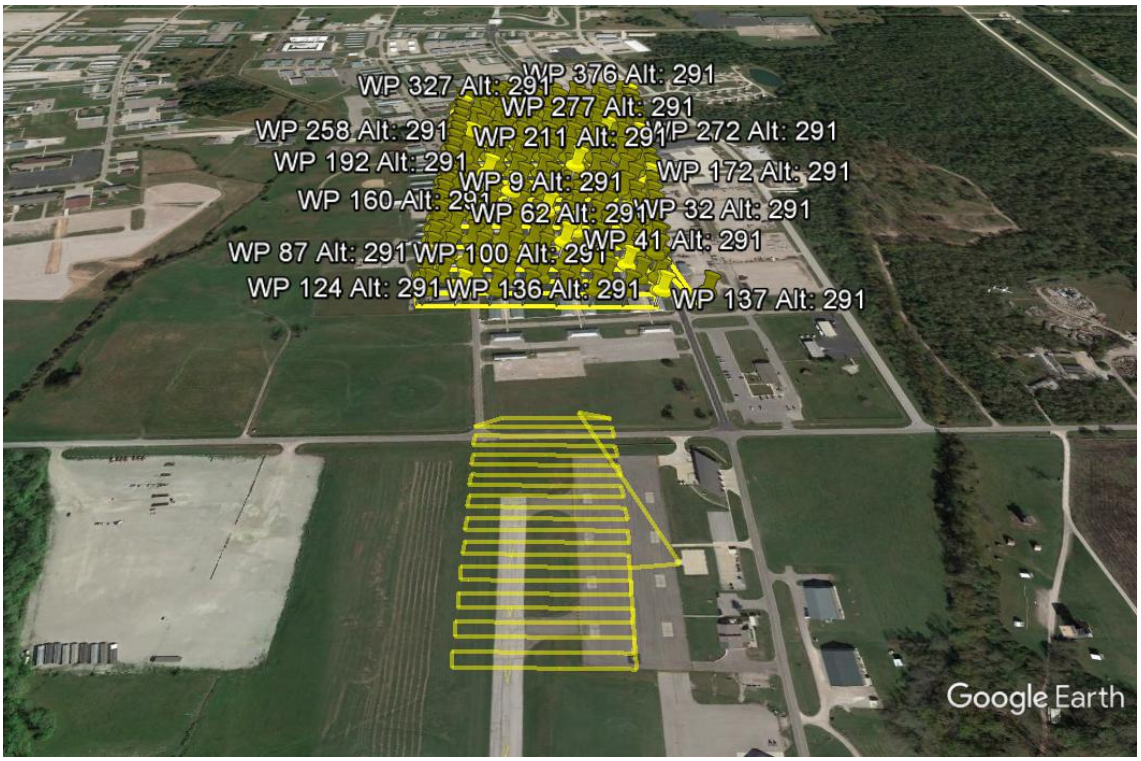

Figure 19: Flight 1A Waypoints

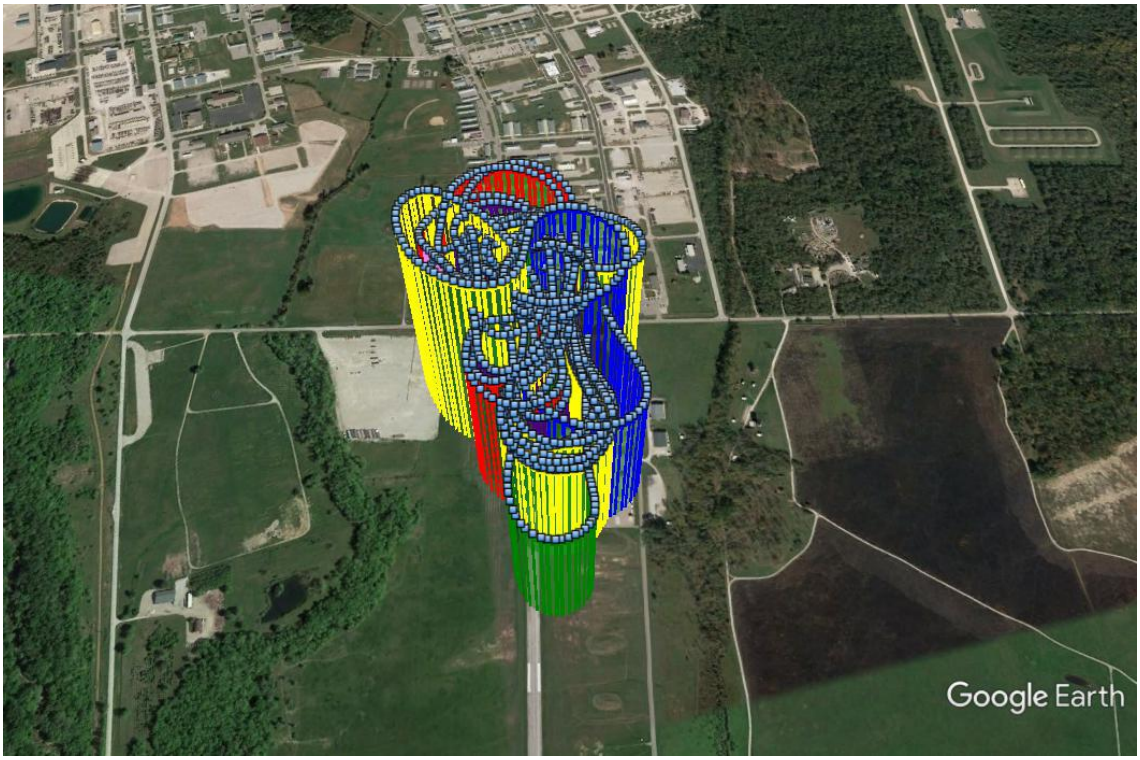

Figure 20: Flight 1A 3D Flight Path

The aerial images from flight 1A were used to generate the orthomosaic shown in Figure 21. The orthomosaic diamond shape does not match the rectangular shape of the

waypoint shown in Figure 19. The orthomosaic diamond shape can be recognized within the flight path illustrated in Figure 20.

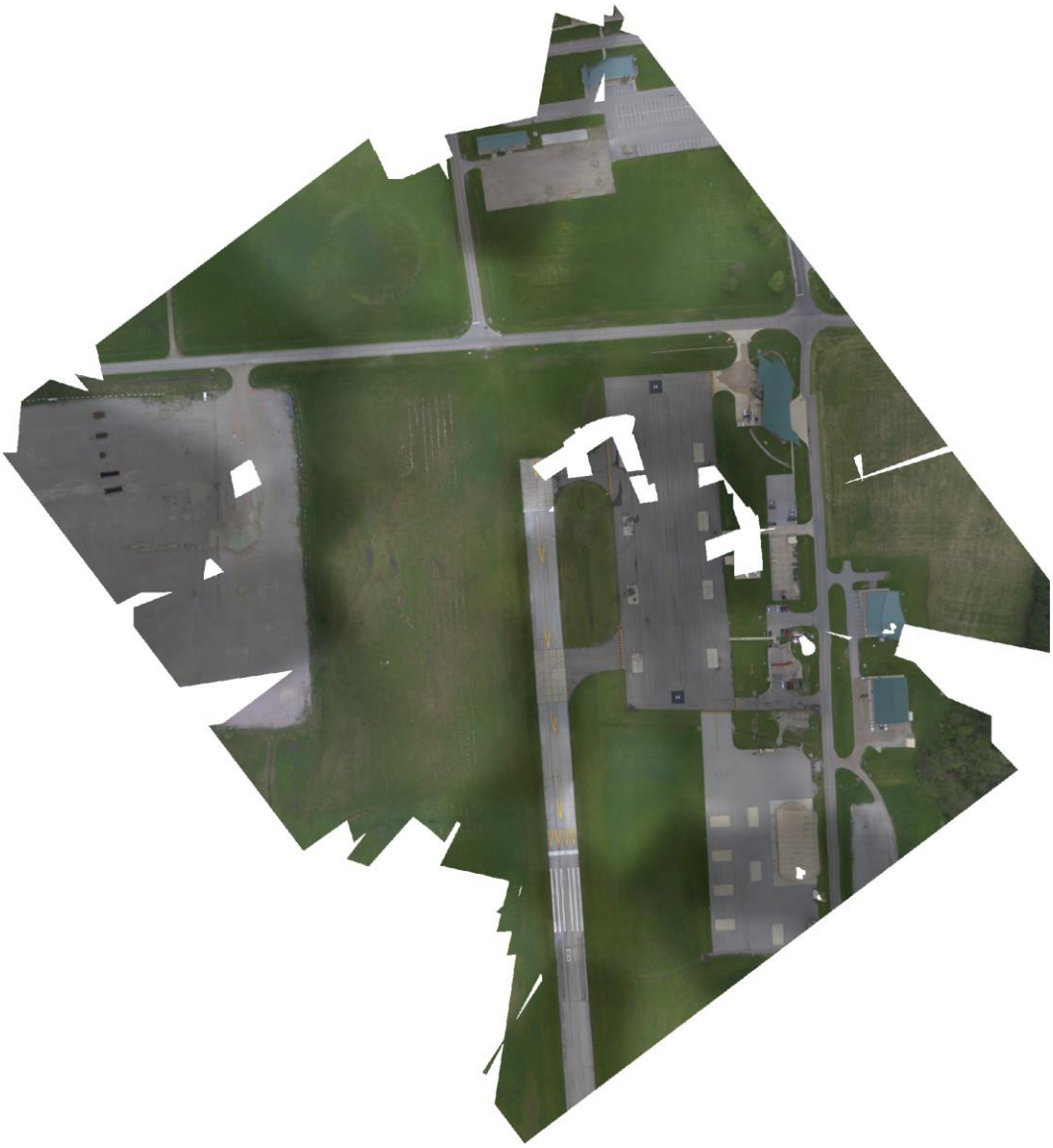

Figure 21: Flight 1A Orthomosaic

The gaps in the orthomosaic are somewhat understandable on the perimeter of the flight pattern. The interior gaps are likely due to not having the recommended overlap

and sidelap. This hypothesis is supported by a study published in the International Journal of Remote Sensing represented in Figure 22 (Ajayi et al, 2017). Ajayi et al. (2017) found that the elevation values found were accurate without the software-recommended overlap and sidelap. The image losses were found to be visually with the orthomosaic and digital elevation model. Ajayi et al. (2017) found their overlap and sidelap values to be in the range of 15-20% for the 92 images captured in manual mode.

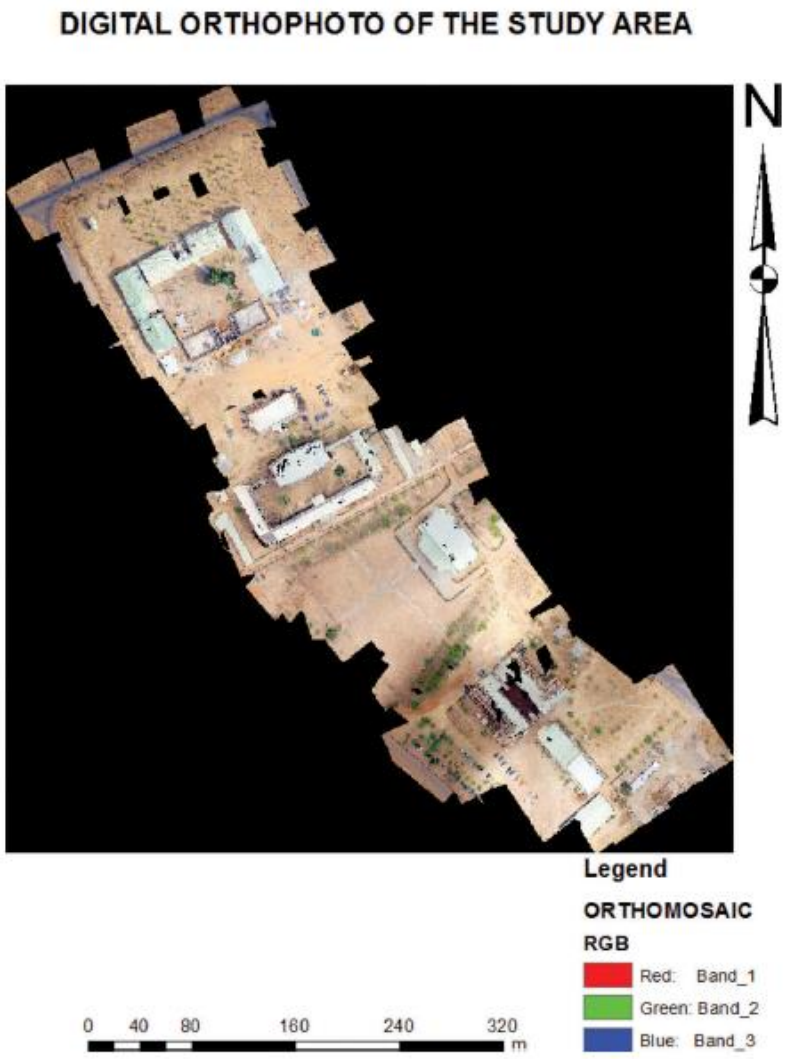

Figure 22: Similar Findings from Low Overlap (Ajayi et al, 2017)

Flight 1B

The aerial images captured proved to be a challenge during alignment during step 2. As shown in Figure 23 only 47 of the 244 images (referred to as cameras in Photoscan) were aligned and they were all tied to the same latitude, longitude, and elevation. That singular point is shown in Figure 23 as the pink sphere.

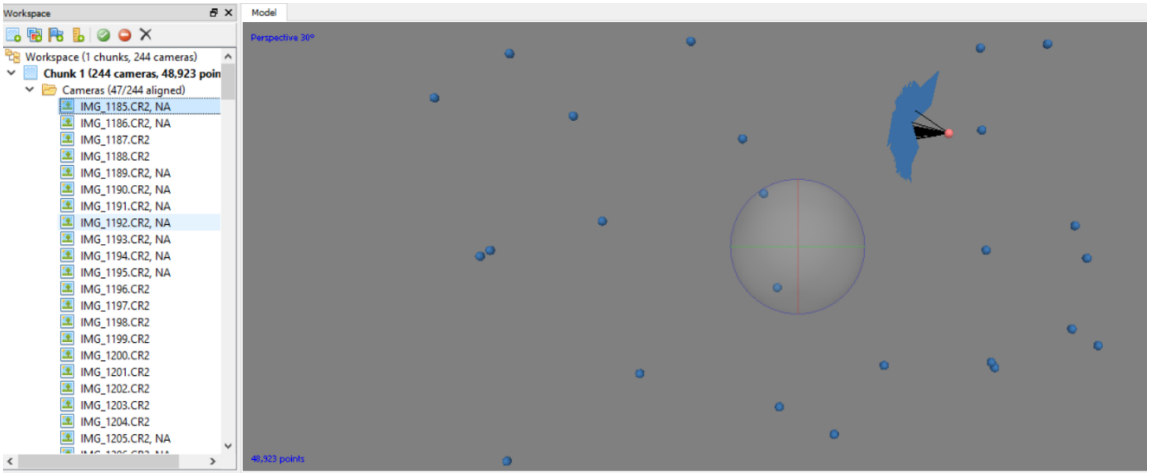

Figure 23: Flight 1B Alignment Difficulty with All Images

Upon further review, 152 image files had the same GPS coordinates. The cause for this is unknown as the remaining 92 images had unique locations as illustrated in Figure 23 by the multiple blue spheres. Multiple attempts were made to eliminate the alignment error to include removing the image files with identical GPS coordinates. Figure 24 shows that this offered only minimal improvement and no orthomosaic was generated from Flight 1B images.

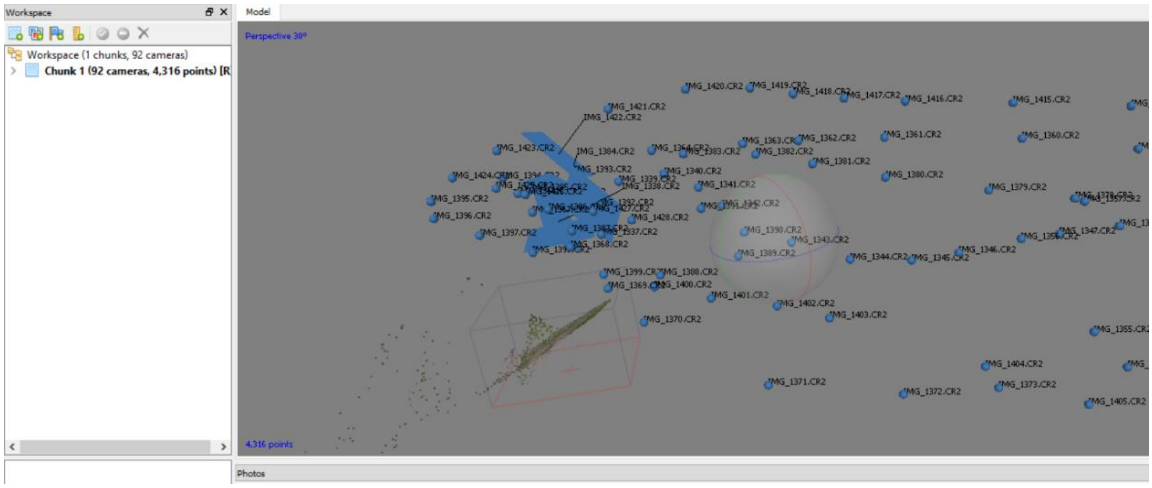

Figure 24: Flight 1B Alignment Difficulty with 92 Images

Flight 1C

An orthomosaic was not possible from the image captured from this flight as the image files did not have the GPS information written to each image as the Canon GPS was not utilized during this portion of the test. Attempts to obtain the GPS locations from the tlog files in Mission Planner were unsuccessful.

Flight 2A

The orthomosaic for Flight 2A is illustrated in Figure 25. The gaps in the image are primarily near the left and right ends of the image, which could be caused by the fact this is where the UAV performed the 180 degree turns to resume the survey over the area of interest. The intervalometer setting for this flight was set at 2 seconds which was calculated after the test to leave 2.2 meters not covered between aerial images. This error could help explain the interior gaps in the image.

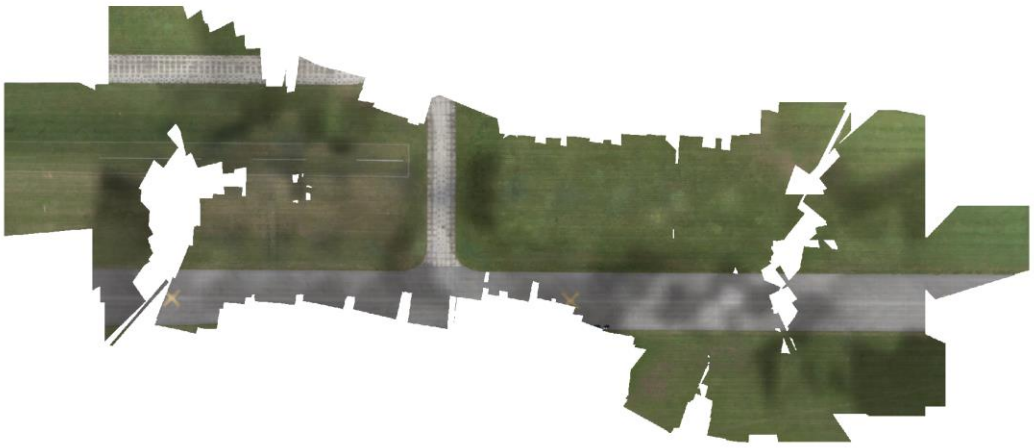

Figure 25: Flight 2A Orthomosaic

Flight 2B

The Flight 2B orthomosaic is shown in Figure 26 and illustrates the challenges Photoscan had when merging the aerial images captured during the turns. The pavement at either end of the image is shown as being askew from the rest of its adjoining pavement.

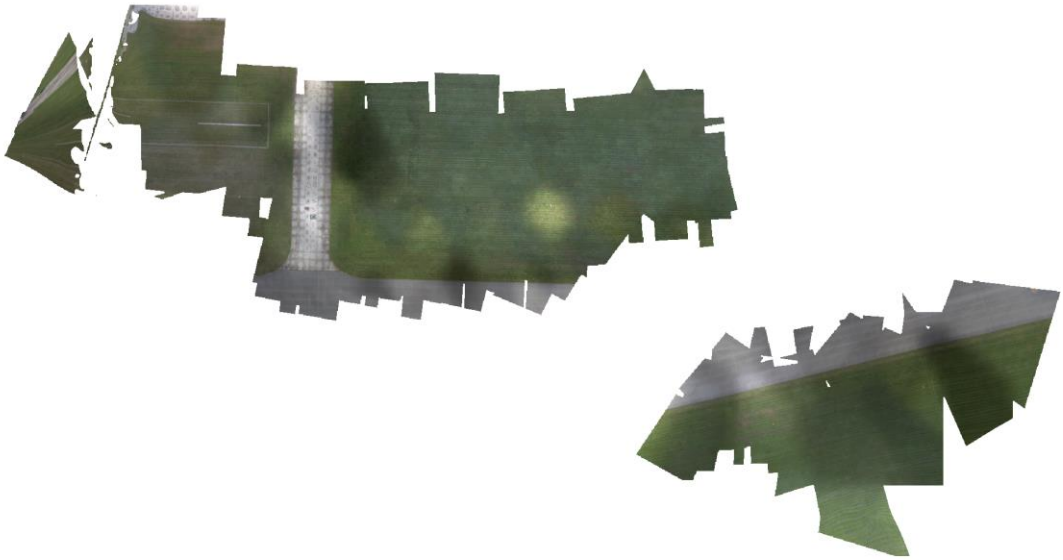

Figure 26: Flight 2B Orthomosaic

Flight 3A

An orthomosaic was not possible as no camera coordinates were available. The Canon GPS was not switched on before flight which was an error by the researcher. Without the camera coordinates, Photoscan could not align the photos.

Flight 3B

The orthomosaic for Flight 3B can be seen in Figure 27 and again shows distress at the turning areas. To ascertain how the orthomosaic would change if those turning aerial images were not included, the bounding box was moved to eliminate those images. The resulting orthomosaic is shown in Figure 28, which is not significantly different visually in both cases, and the ground resolution proved to be the same (6.53 mm) as shown in Table 11.

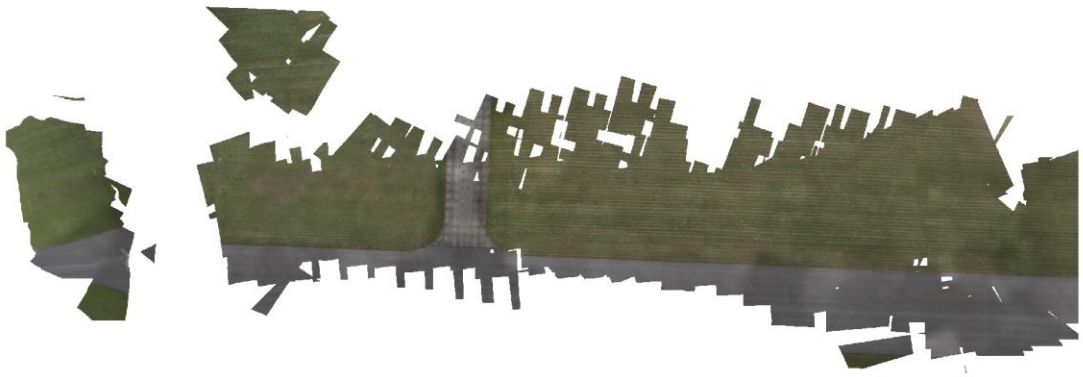

Figure 27: Flight 3B Orthomosaic

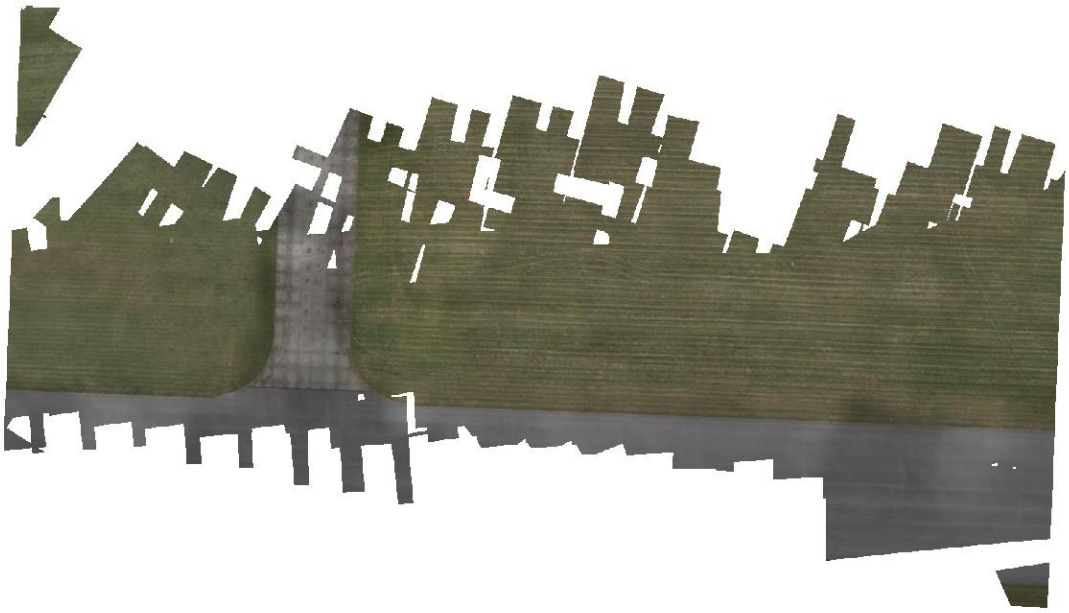

Figure 28: Flight 3B Orthomosaic Bounded

Test Article Measurement

One of the measurements from the Flight 2B was the radius/diameter of the test ring in the orthomosaic. After merging dozens of photos together, would a 96" diameter circle still be represented as a 96" diameter circle? The radius value measured within Google Earth was 48" as shown in Figure 29. Figure 30 shows the test ring measured with a physical tape measure.

Figure 29: Flight 2B 8' Dirt Ring Verification

Figure 30: Test Ring Measured Diameter Approximately 96” with Tape Measure

The ground resolution displayed in Figure 29 led to the decision to lower the flight altitude from 60 meters flown in Flight 2 to 32 meters flown in Flight 3. More detail was needed to identify and measure the test articles.

The 2” x 3” pipe section was also measured from the orthomosaic. Figure 31 shows the measured length values in both Google Earth (GE) and Photoscan. The units default to metric, but the conversion of the 8.84 cm length in GE is equal to 3.48 in and the 7.65 cm via Photoscan is equal to 3.01 in.

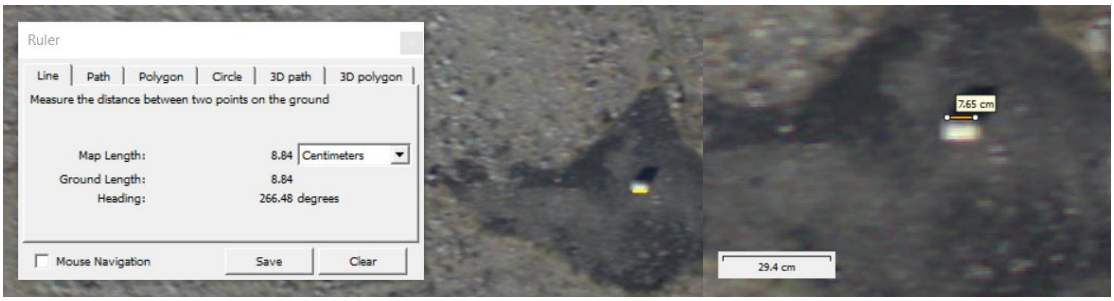

Figure 31: Flight 3B Measured Length of 2” x 3” Test Article GE left, Photoscan right

Figure 32 shows the test article diameter which was found to be 4.79 cm in GE which converts to 1.89 in and the Photoscan measurement of 4.71 cm or 1.85 in.

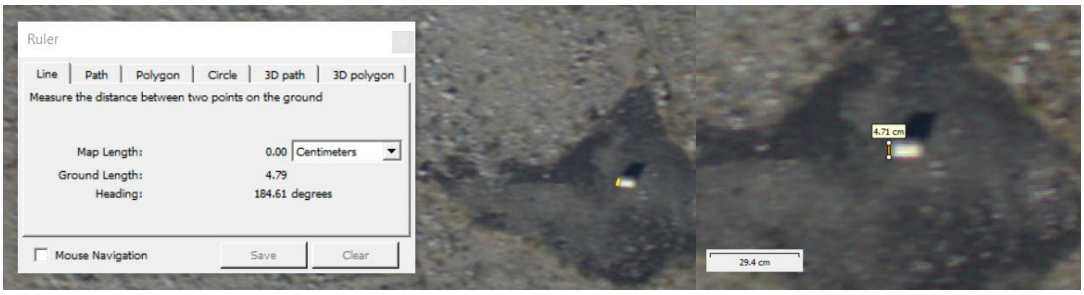

Figure 32: Flight 3B Measured Diameter of 2" x 3" Test Article GE left, Photoscan right

The ground truth of the 2" x 3" test article is shown in Figure 33.

Figure 33: 2" by 3" Pipe Section Length and Diameter Measured with Tape Measure

The measured values are listed in Table 8 for the smallest pipe section. It was challenging to define and select the test article edges consistently within the software. The lack of consistency eliminated the ability to perform a comparative statistical analysis via root-mean-square error. The orthomosaic measured values in both Google Earth and Photoscan were shown to be consistent.

Table 8: 2” by 3” Test Article Measurements

	Length	Diameter
Google Earth	3.48"	1.89"
Photoscan	3.01"	1.85"
Ground truth	3.13"	2.25"

The 3” x 8” pipe section length was found to be 23.76 cm in GE which converts to 9.35 in while the Photoscan value was found to be 21 cm or 8.27 in as shown in Figure 34.

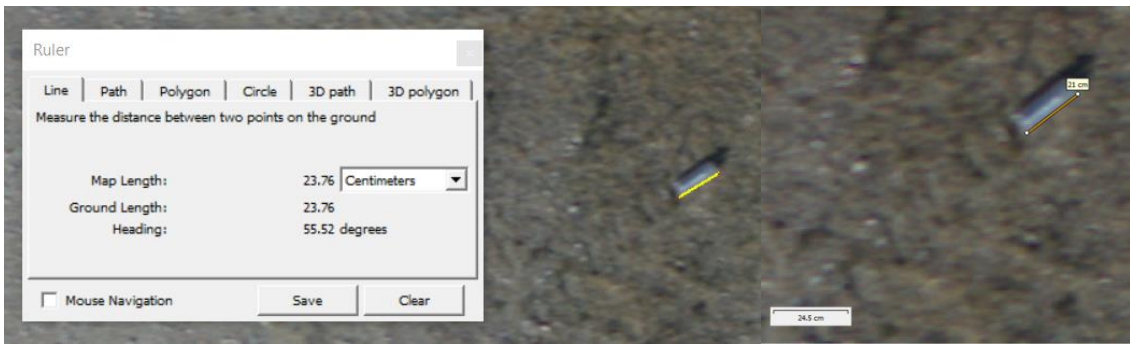

Figure 34: Flight 3B Measured Length of 3” x 8” Test Article GE left, Photoscan right

The diameter of the 3” x 8” test article was found to be 7.74 cm in GE which equals 3.05 in and 7.55 cm in Photoscan which is 2.97 in as shown in Figure 35.

Figure 35: Flight 3B Measured Diameter of 3” x 8” Test Article GE left, Photoscan right

The ground truth of the 3” x 8” test article is shown in Figure 36 and all values are listed in Table 9.

Figure 36: 3” by 8” pipe section length and diameter measured with tape measure

Table 9: 3” by 8” Test Article Measurements

	Length	Diameter
Google Earth	9.35"	3.05"
Photoscan	8.27"	2.97"
Ground truth	8.13"	2.94"

The 8” x 20” pipe section length was found to be 50.81 cm in GE which converts to 20.00” and Photoscan found 50.9 cm which is equivalent to 20.04 in. These values are shown in Figure 37.

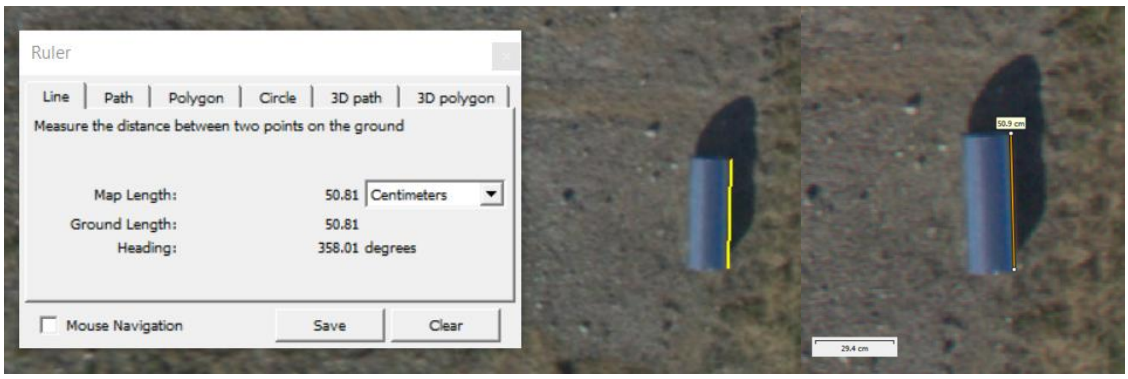

Figure 37: Flight 3B Measured Length of 8” x 20” Test Article GE left, Photoscan right

The diameter of the 8” x 20” was measured on the orthomosaic in GE at 17.69 cm which is 6.96 in and Photoscan was 18.8 cm or 7.40” as shown in Figure 38.

Figure 38: Flight 3B Measured Width of 8” x 20” Test Article GE left, Photoscan right

The ground truth of the 8” x 20” test article is shown in Figure 39 and all values are listed in Table 10.

Figure 39: 8” by 20” Pipe Section Length and Diameter Measured with Tape Measure

Table 10: 8” x 20” Test Article Measurements

	Length	Diameter
Google Earth	20.00"	6.96"
Photoscan	20.04"	7.40"
Ground truth	20"	7.75"

Digital Elevation Model Flight 3B

Figure 40 highlights the level of detail obtained in the digital elevation model (DEM) produced from the images obtained in flight 3B. Figure 40 shows the area of interest border along the grass in the orthomosaic and DEM layers. The grass height was previously measured by the researcher to be 8" tall along the vertical edge shown on the right side of the image, as shown in Figure 42. The 8" by 20" test article running vertically in the figure along the grass line height above ground was 6.75". Both the grass line and 8" by 20" test article are represented in the DEM.

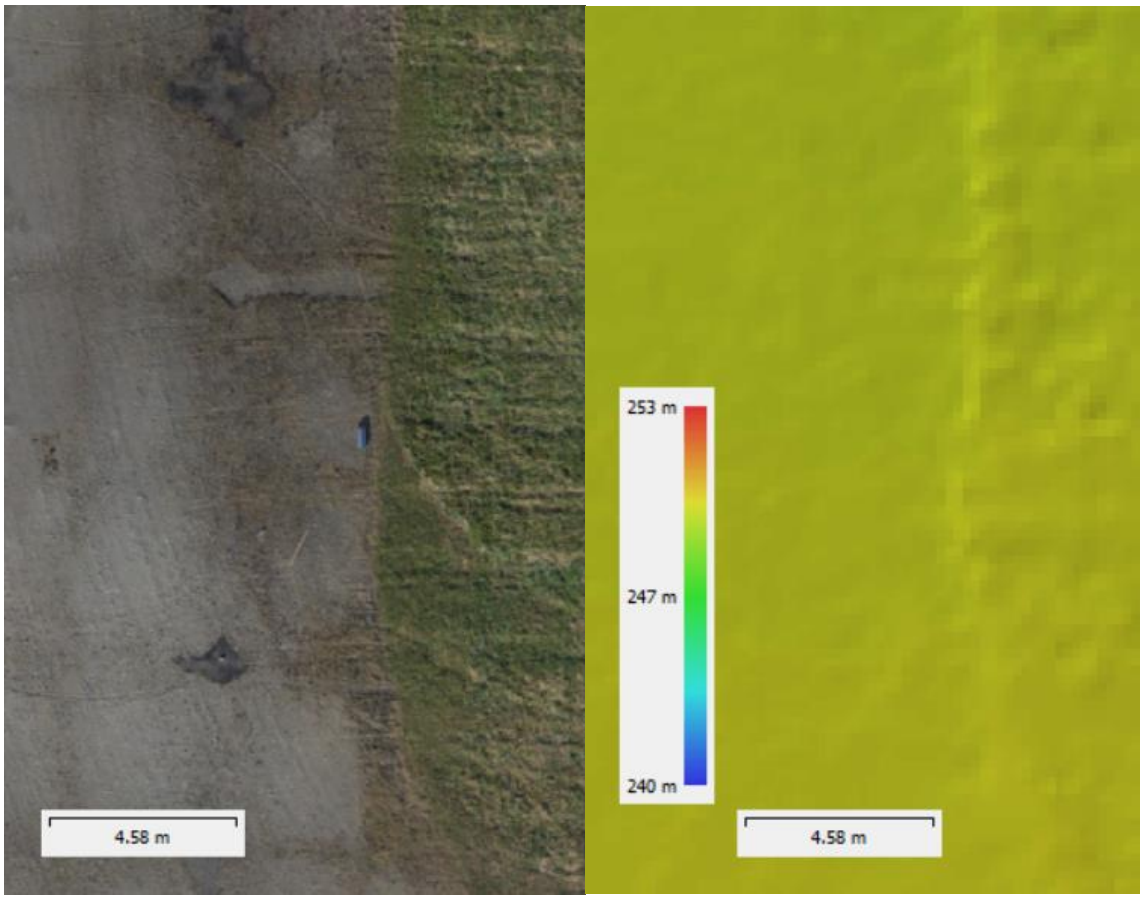

Figure 40: Flight 3B Area of Interest Orthomosaic on left, DEM on right

The Montgomery County Engineer's office provides details of the dozens of geodetic points across the county. The WPAFB Area B airfield is within Montgomery County; although there was not a point on the airfield there was one nearby as shown in Figure 41. The average GPS elevation is listed at 810.39 feet or 247.01 meters which is in line with the digital elevation model shown in Figure 40 with 247 meters listed at the midpoint of the scale.

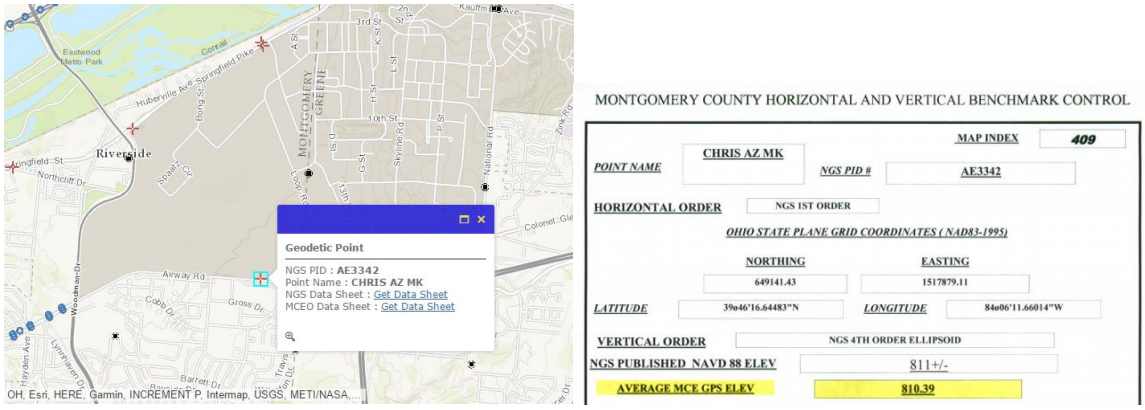

Figure 41: Elevation Value from Montgomery County Engineer's Office Geodetic Control (http://engineer.gomvo.org/apps/GeodeticControl/)

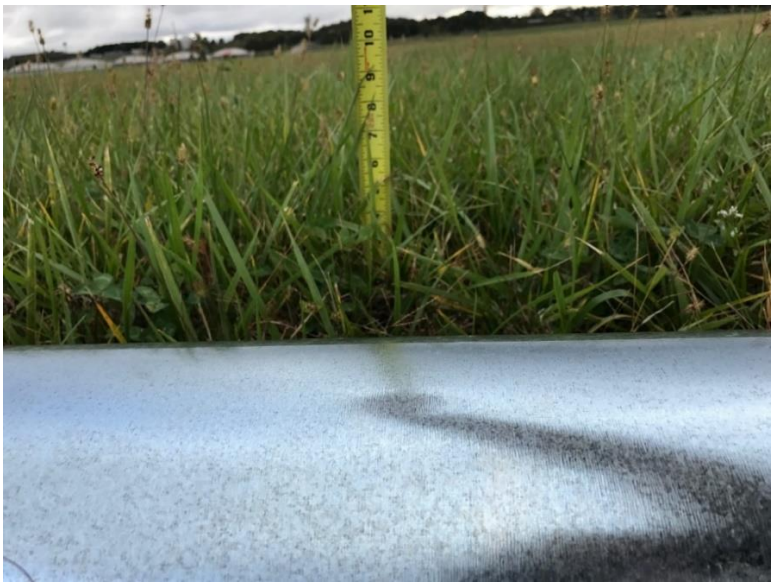

Figure 42: Grass Height in October 2016 Four Weeks Before Flight 3B

GPS Comparison Canon versus Pixhawk

Flights 1A and 1B provided a means to compare both the camera and autopilot GPS as there was a question as to which would be more accurate. Figures 43 and 44 explore the information available from the tlog file generated by Mission Planner for each flight. The blue and purple asterisks indicate the GPS position of the Pixhawk and Canon GPS, respectively, when an aerial image was captured. Visually, the points are in a similar location or overlay one another, which is what one would expect of two similar grade GPS receivers in the same UAV.

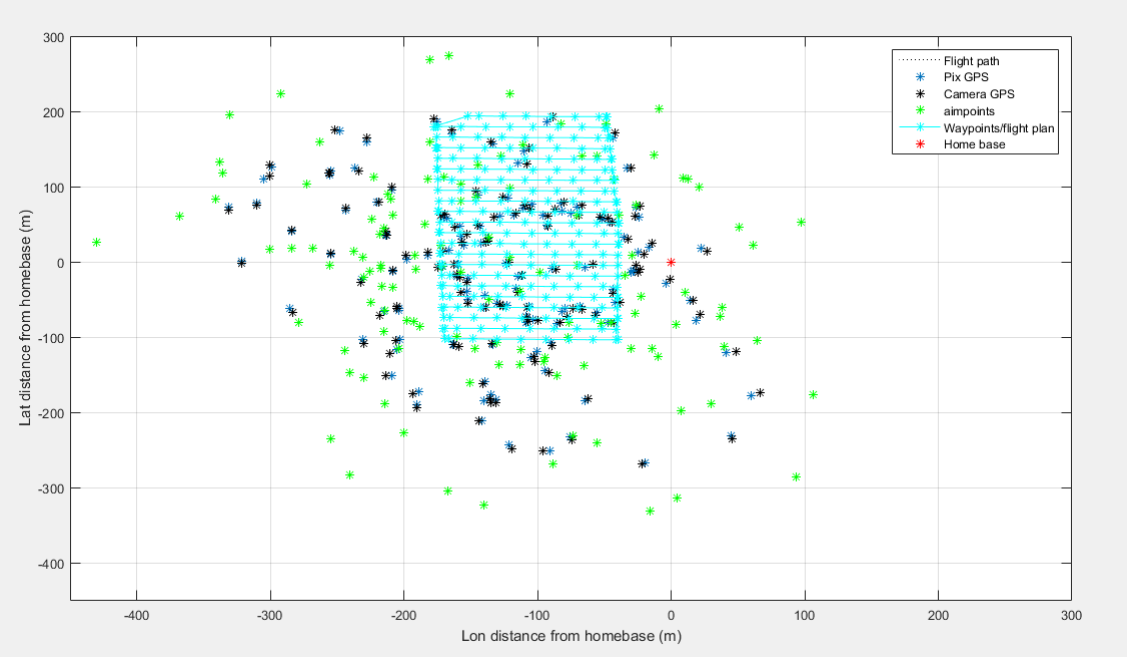

Figure 43: Flight 1A Pixhawk and Canon GPS Image Locations

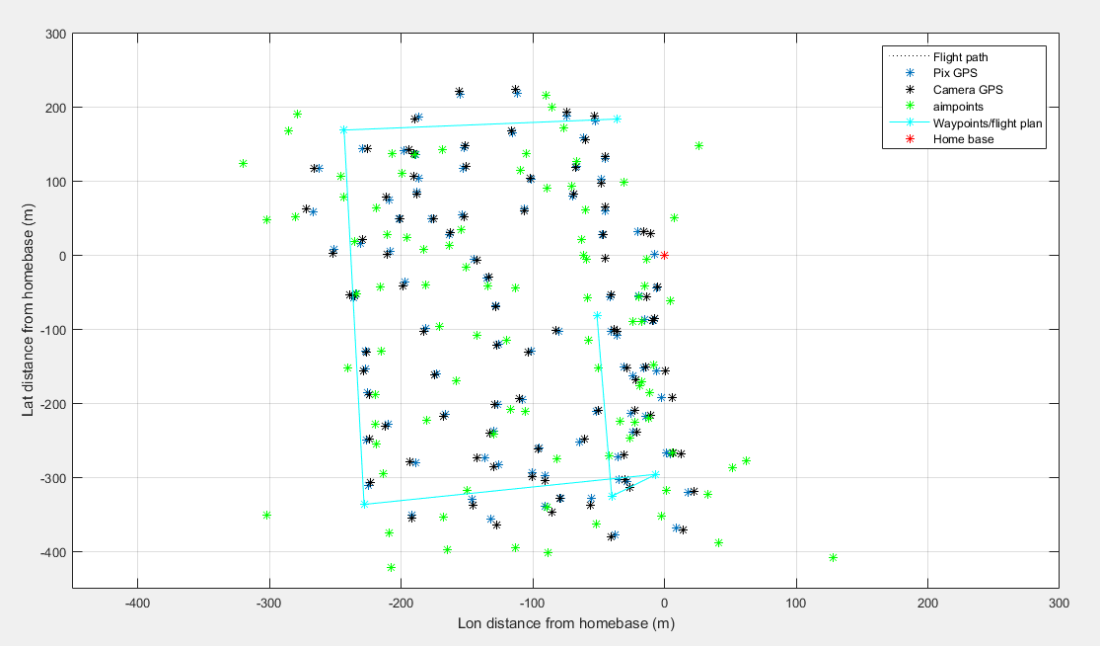

Figure 44: Flight 1B Pixhawk and Canon GPS Image locations

Inserting orthomosaic into Google Earth

Google Earth provides a means to view the orthomosaic overlaid onto a satellite image. At first glance, it appears that the orthomosaic was wrongly placed as shown in Figure 45. When another satellite version was selected, the shift was made to the other side as shown in Figure 46. Google Earth has multiple satellite images available dating back to 1994, which can be useful when comparing changes to an area over time. Error in GPS of the plane and camera could contribute to variations in matching Google Earth satellite imagery.

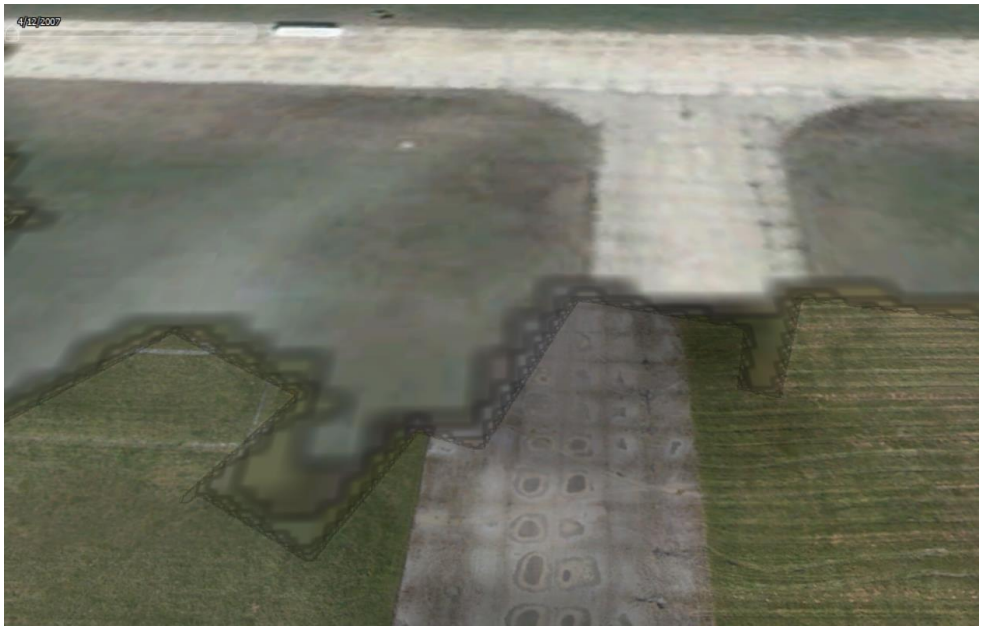

Figure 45: Error Between Flight 3B Orthomosaic and 2007 Google Earth Satellite

Figure 46: Error Between Flight 3B Orthomosaic and 2016 Google Earth Satellite

Photoscan Comparison

During the image alignment step in Photoscan one has an option of selecting Highest or High for processing. The aerial images captured in Flights 2B and 3B were run in each of the settings to compare the results. The three metrics compared were processing time, ground resolution, and reprojection error. Table 11 shows the results which indicate that the High setting took less time to produce better ground resolution. The Highest setting may perform better in an area with more elevation variety. The laptop used to process the images had an Intel Core i7-6700HQ CPU @ 2.60GHz processor, 32 GB of RAM, and a 459 GB hard drive.

Table 11: Photoscan Alignment Accuracy Setting Comparison

Processing Time	
Flight 2B Images Highest Setting	22 min 3 sec
Flight 2B Images High Setting	17 min 23 sec
Flight 3B Images Highest Setting	61 min 47 sec
Flight 3B Images High Setting	49 min 17 sec
Ground Resolution	
Flight 2B Images Highest Setting	1.14 cm/pix
Flight 2B Images High Setting	1.11 cm/pix
Flight 3B Images Highest Setting	6.61 mm/pix
Flight 3B Images High Setting	6.53 mm/pix
Reprojection Error	
Flight 2B Images Highest Setting	0.953 pix
Flight 2B Images High Setting	0.928 pix
Flight 3B Images Highest Setting	0.758 pix
Flight 3B Images High Setting	0.752 pix

The increase in ground resolution as the altitude was changed from 60 meters to 32 meters can be seen in Table 12. The predicted ground resolution from Mission

Planner for the individual aerial images are also listed, which is slightly better than the orthomosaic generated by Photoscan. Minimal impact was seen in ground resolution difference when the bounding box was utilized. The bounding box allows for those images captured while the UAV is turning to be eliminated from the orthomosaic.

Table 12: Ground Resolution Comparisons

Flight 2B (60 m)		Ground resolution
Mission Planner	(individual images)	10.8 mm
Photoscan	(orthomosaic)	11.1 mm
Bounding Box		10.6 mm

Flight 3B (32 m)		Ground resolution
Mission Planner	(individual images)	5.7 mm
Photoscan	(orthomosaic)	6.53 mm
Bounding Box		6.53 mm

Applied Analysis

This research focused on a specific area of interest within an airfield. AFCEC's focus is to address an entire runway that was attacked. An accurate representation as to the size and location of damage incurred and the location of any unexploded ordnance is the first step to returning to service. The amount of time required for Photoscan to process the aerial images into an orthomosaic is evaluate in Figure 47. Time in seconds are on the vertical axis and the number of aerial images in each of the four flights an orthomosaic was generated. A trendline was fit to allow one to estimate the orthomosaic processing time for a full runway.

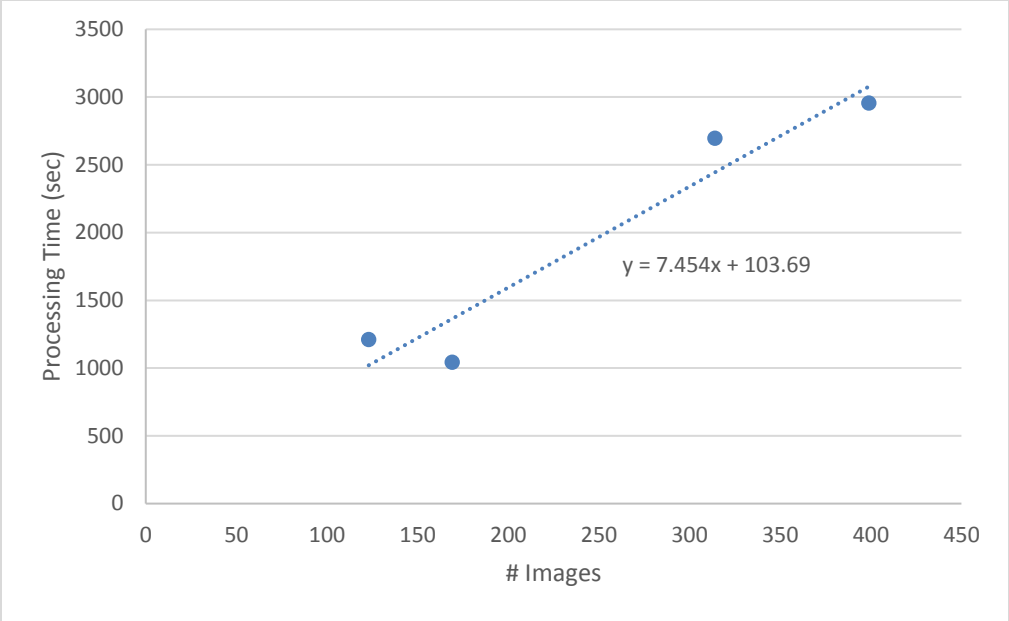

Figure 47: Processing Time vs Image Total

Consider a runway 10,000 feet long and 150 feet wide being surveyed by the same UAS used in this research at an altitude of 32 meters. With 80% forward overlap one can determine the amount of images required per row. 10,000 feet is equal to 3,048 meters which divided by the vertical dimension of the image area of 20.18 meters multiplied by 20% equals 4.03 meters of new ground covered with each image. Dividing the runway length of 3,048 meters by 4.03 meters equals 756.33 images per row. The number of rows required is determined by the 60% sidelap which allows for 40% of the horizontal dimension of the image area to be covered per row. 40% multiplied by 23.82 meters equals 9.53 meters which divides the 45.72 meter width into 4.8 rows. 756.33 images per row multiplied by 4.8 rows equals 3,630.38 images. Using the trendline equation from Figure 47, the projected estimate for orthomosaic processing time required is 427.74 minutes. Another factor to consider is the amount of storage space required for

3,630.38 images. Considering a 25 MB average per aerial image, 90,759.5 MB of storage will be required. One will also need to make allowances if images are captured before starting the survey, during the turns, and after completing the survey.

Investigative Questions Answered

The goal of this research was to explore the capabilities of current commercial UAVs, cameras, and software to provide decision makers with more accurate information than they have had before in a timely manner. This research focused on airfields and the ability to represent current conditions.

1. **How can imagery from a COTS UAS be beneficial to a civil engineer squadron?**

This research has shown that a UAS is capable of capturing high resolution images of an airfield which can then be processed into a singular mosaic without a significant loss of resolution. The resulting orthomosaic can then be viewed in position on a satellite image which allows for location latitude and longitude. Unfortunately the accuracy of this location could not be verified with the flight tests performed. Repeatability was demonstrated with multiple flights although challenges were experienced and documented.

2. **What flight and processing methods provide the best orthomosaic resolution and accuracy?**

This research found that the lower altitude produced higher ground resolution images and the orthomosaic had a lower reprojection error. The challenge at the lower

altitude was being able to maintain the suggested forward overlap percentage. Adjusting the Mission Planner survey settings to include overshoot and lead-in waypoints helped the UAV cover the area of interest more consistently.

This research found that ground resolution and dimensional accuracy can be maintained in an orthomosaic with minimal loss. The digital elevation model proved to be accurate based on survey data in the area and was able to distinguish height differences of less than 12 inches.

Summary

This chapter presented the results of flight tests, image processing, and orthomosaic accuracy for four flights at two locations. Comparisons were made between the predicted and actual ground resolution values. The test articles were also measured and compared to their actual dimensions. An aerial orthomosaic offers a significant improvement as to how pavement condition is currently represented. The following chapter presents an interpretation and conclusion to these findings.

V. Conclusions and Recommendations

Chapter Overview

This chapter discusses and interprets the results presented in this research. Conclusions will be reached based upon findings and potential for use by civil engineer squadrons. Potential follow on opportunities will also be discussed.

Conclusions of Research

This research shows that a low-cost COTS fixed-wing UAS is possible of capturing images with ground resolution of less than 6 mm/pixel. Commercial software is available that can maintain the ground resolution while merging hundreds of individual images into one orthomosaic and digital elevation model. The visual representation of the area of interest is a valuable one that can provide accurate dimensions and relative location. Being able to capture an airfield's condition digitally from an aerial viewpoint is a dramatic improvement to an subjective 0-100 point scale or tri-color sketch.

Recommendations for Action

Consider a report of suspicious objects on the airfield. Figure 48 provides an example of the differences in perspective. While both images show the same four test articles and were taken at relatively the same time, there is a large difference in the ability to locate, identify, and measure them. Individual snapshots are unable to canvas an area to provide the big picture. A mosaic allows for an expert to focus on objects of interest while having a large perspective. Having personnel hundreds of feet away as opposed to ten feet provides personnel safety.

Figure 48: Ground Level Image of Test Articles top, Flight 3B Orthomosaic of Test Articles (32m altitude) bottom

There are commercial products available today that can provide an installation better information which should lead to better decisions. These decisions can range from non-emergency applications such as airfield pavement maintenance to emergency applications such as disaster response.

Recommendations for Future Research

There are numerous options for future studies that became clear after performing this research. The ability to verify position accuracy could be evaluated with ground control points. While the elevation of the digital elevation model was similar to a geodetic point outside the airfield, it would be interesting to verify the GPS location of a point within the orthomosaic beyond Google Earth. The possibility of integrating the orthomosaic into GeoBase, the AF geographic information system (GIS), would be the best way to capture and transfer the valuable information beyond the squadron. This could be another way to verify the actual orthomosaic position as challenges were found in Google Earth between satellite images. Capturing images after a rain to measure ponding, rutting, etc., would be a unique possibility offered if one had a UAS at hand. Rotating the camera 90 degrees to allow for more forward overlap would be one way to combat the image area lost when lowering altitude. Exploring the possibility of being able to determine which individual images cover a point in an orthomosaic or digital elevation model would be an interesting capability. Comparing different software packages for image processing and comparing the resulting values from orthomosaic generation. Flight testing was found to be more effective as a team as opposed to one individual. Perhaps a pair of researchers could work together to capture images and then

work independently on processing. Pairing researchers for flight testing to help with checklists, initial data review, and flight test plan review.

Summary

UAVs offer the ability to move from analog inspection to a digital one. Stitching software can take hundreds of seemingly scattered and isolated images across an area and generate a single overhead view. Being able to accurately capture and communicate the condition of acres of pavement is crucial to the AF primary mission. With many secondary benefits of such a system, the minimal cost is justifiable.

Appendix A. Flight 1A Report

Agisoft PhotoScan Flight 1A

Processing Report
22 February 2017

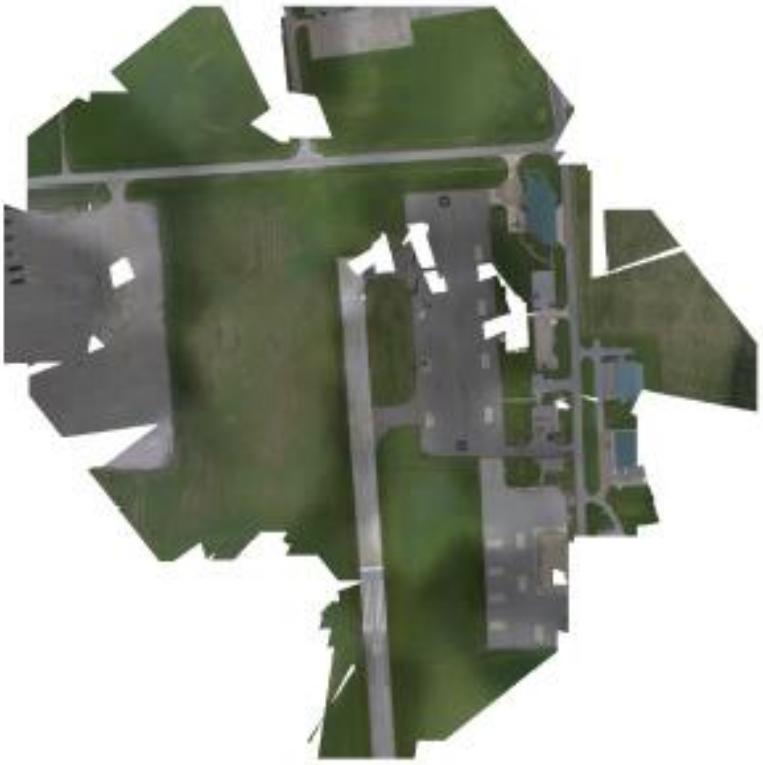

Survey Data

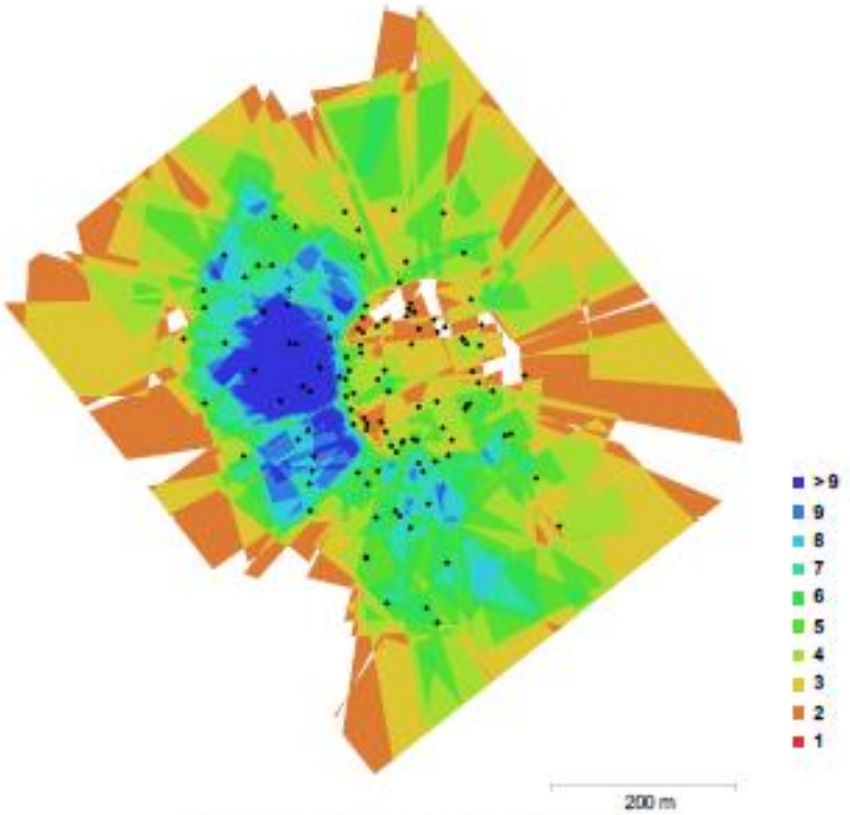

Fig. 1. Camera locations and image overlap.

Number of images:	123	Camera stations:	116
Flying altitude:	127 m	Tie points:	263,825
Ground resolution:	2.22 cm/pix	Projections:	732,679
Coverage area:	0.323 km²	Reprojection error:	0.92 pix

Camera Model	Resolution	Focal Length	Pixel Size	Precalibrated
Canon EOS REBEL SL1 (24 mm)	5184 x 3456	24 mm	4.38 x 4.38 µm	No

Table 1. Cameras.

Camera Calibration

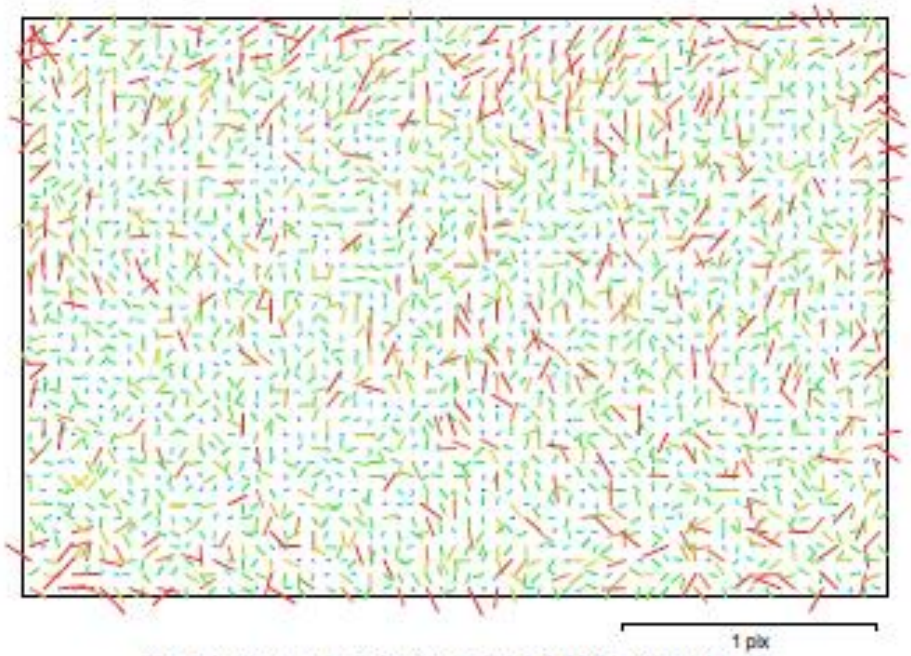

Fig. 2. Image residuals for Canon EOS REBEL SL1 (24 mm).

Canon EOS REBEL SL1 (24 mm)

123 images

Resolution	Focal Length	Pixel Size	Precalibrated
5184 x 3456	**24 mm**	**4.38 x 4.38 µm**	**No**

Type:	Frame	F:	5705.19
Cx:	-32.638	B1:	-2.83124
Cy:	35.6753	B2:	0.562754
K1:	-0.12761	P1:	-0.000602201
K2:	0.135019	P2:	0.000623966
K3:	0	P3:	0
K4:	0	P4:	0

Camera Locations

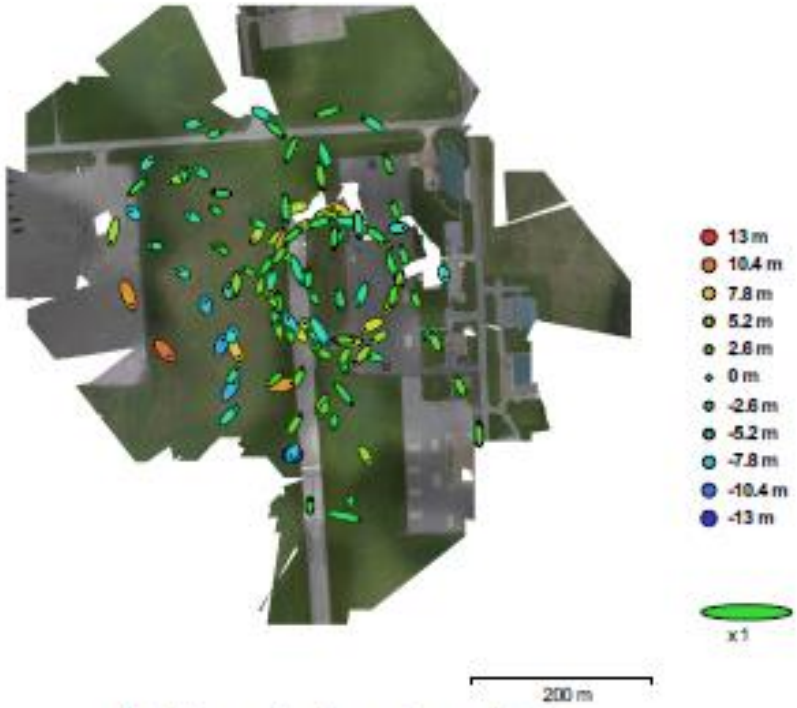

Fig. 3. Camera locations and error estimates.
Z error is represented by ellipse color. X,Y errors are represented by ellipse shape.
Estimated camera locations are marked with a black dot.

X error (m)	Y error (m)	Z error (m)	XY error (m)	Total error (m)
10.0036	12.4044	4.09005	15.9356	16.4521

Table 2. Average camera location error.

Digital Elevation Model

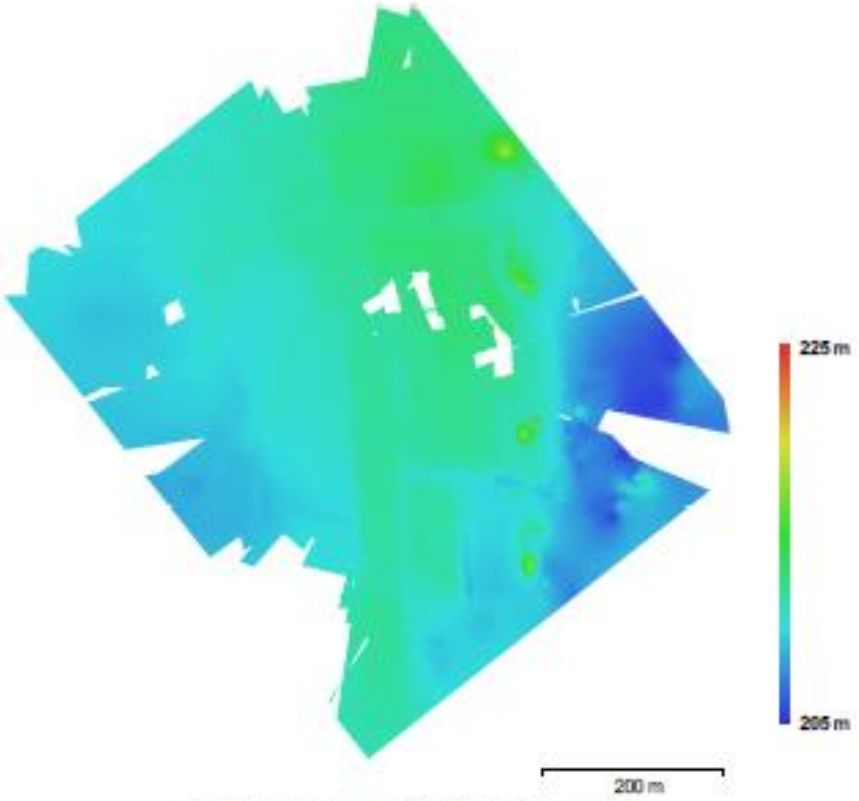

Fig. 4. Reconstructed digital elevation model.

Resolution:	71 cm/pix
Point density:	1.98 points/m²

Processing Parameters

General	
Cameras	123
Aligned cameras	116
Coordinate system	WGS 84 (EPSG::4326)
Point Cloud	
Points	263,825 of 288,891
RMS reprojection error	0.121496 (0.919831 pix)
Max reprojection error	0.366609 (22.7642 pix)
Mean key point size	7.19284 pix
Effective overlap	2.85632
Alignment parameters	
Accuracy	High
Pair preselection	Reference
Key point limit	40,000
Tie point limit	10,000
Constrain features by mask	No
Adaptive camera model fitting	Yes
Matching time	10 minutes 55 seconds
Alignment time	2 minutes 49 seconds
DEM	
Size	1,186 x 1,212
Coordinate system	WGS 84 (EPSG::4326)
Reconstruction parameters	
Source data	Sparse cloud
Interpolation	Enabled
Processing time	2 seconds
Orthomosaic	
Size	35,846 x 37,127
Coordinate system	WGS 84 (EPSG::4326)
Channels	3, uint8
Blending mode	Mosaic
Reconstruction parameters	
Surface	DEM
Enable color correction	No
Processing time	6 minutes 26 seconds
Software	
Version	1.2.6 build 2834
Platform	Windows 64 bit

Appendix B. Flight 2A Report

Agisoft PhotoScan Flight 2A

Processing Report
06 March 2017

Survey Data

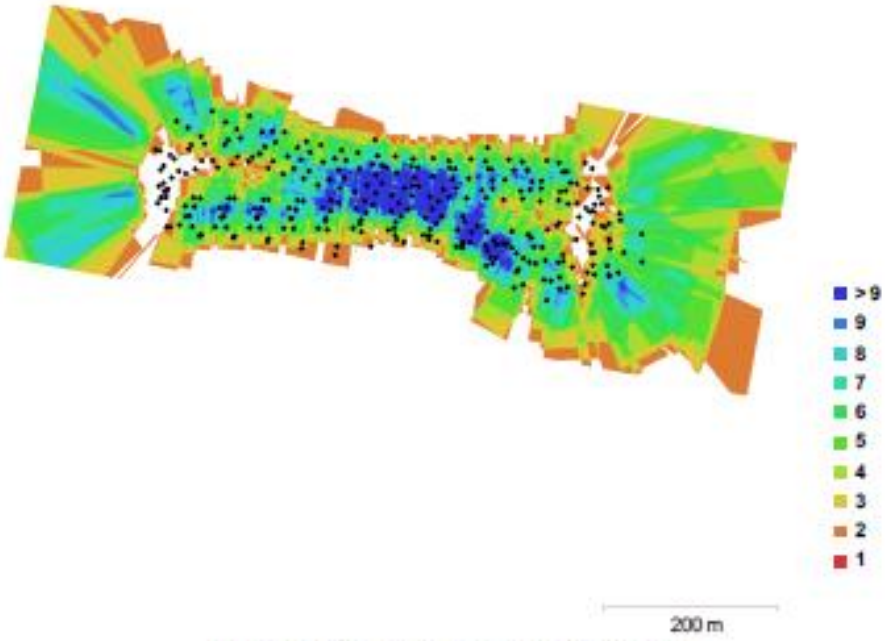

Fig. 1. Camera locations and image overlap.

Number of images:	314	Camera stations:	305
Flying altitude:	65.7 m	Tie points:	755,287
Ground resolution:	1.14 cm/pix	Projections:	2,360,840
Coverage area:	0.192 km²	Reprojection error:	0.872 pix

Camera Model	Resolution	Focal Length	Pixel Size	Precalibrated
Canon EOS REBEL SL1 (24 mm)	5184 x 3456	24 mm	4.38 x 4.38 µm	No

Table 1. Cameras.

Camera Calibration

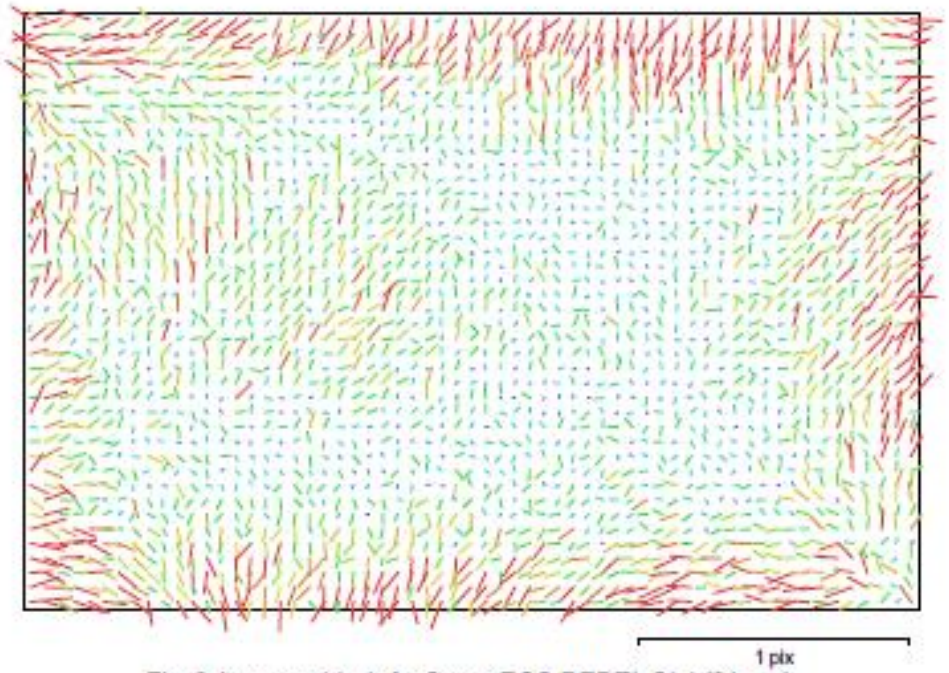

Fig. 2. Image residuals for Canon EOS REBEL SL1 (24 mm).

Canon EOS REBEL SL1 (24 mm)

314 images

Resolution	Focal Length	Pixel Size	Precalibrated
5184 x 3456	**24 mm**	**4.38 x 4.38 µm**	**No**

Type:	Frame	F:	5757.65
Cx:	-30.6053	B1:	-5.37019
Cy:	38.2263	B2:	1.18517
K1:	-0.12872	P1:	-0.000552749
K2:	0.13453	P2:	0.000562811
K3:	0	P3:	0
K4:	0	P4:	0

Camera Locations

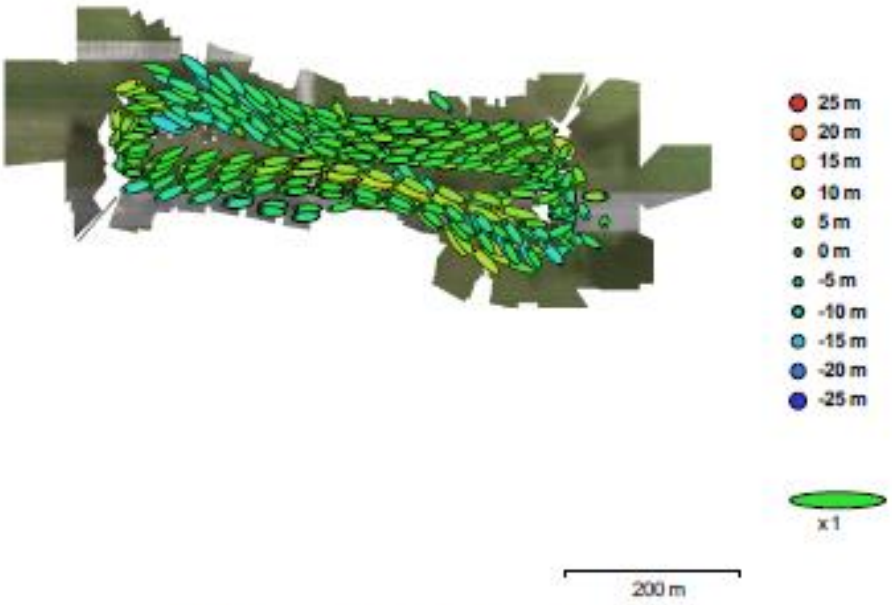

Fig. 3. Camera locations and error estimates.
Z error is represented by ellipse color. X,Y errors are represented by ellipse shape.
Estimated camera locations are marked with a black dot.

X error (m)	Y error (m)	Z error (m)	XY error (m)	Total error (m)
24.7701	12.8794	5.23646	27.9184	28.4052

Table 2. Average camera location error.

Digital Elevation Model

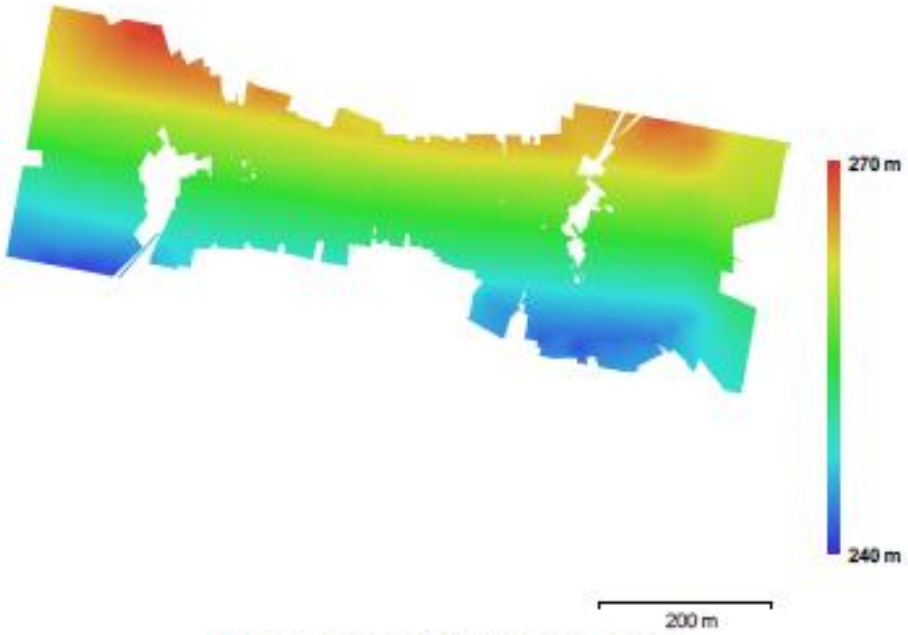

Fig. 4. Reconstructed digital elevation model.

Resolution:	32.6 cm/pix
Point density:	9.42 points/m²

Processing Parameters

General	
Cameras	314
Aligned cameras	305
Coordinate system	WGS 84 (EPSG::4326)
Point Cloud	
Points	755,287 of 800,197
RMS reprojection error	0.146424 (0.871634 pix)
Max reprojection error	0.440474 (30.6369 pix)
Mean keypoint size	5.9019 pix
Effective overlap	3.21041
Alignment parameters	
Accuracy	High
Pair preselection	Reference
Key point limit	40,000
Tie point limit	10,000
Constrain features by mask	No
Adaptive camera model fitting	Yes
Matching time	25 minutes 50 seconds
Alignment time	6 minutes 17 seconds
DEM	
Size	2,830 x 1,402
Coordinate system	WGS 84 (EPSG::4326)
Reconstruction parameters	
Source data	Sparse cloud
Interpolation	Enabled
Processing time	7 seconds
Orthomosaic	
Size	80,861 x 40,059
Coordinate system	WGS 84 (EPSG::4326)
Channels	3, uint8
Blending mode	Mosaic
Reconstruction parameters	
Surface	DEM
Enable color correction	No
Processing time	12 minutes 49 seconds
Software	
Version	1.2.6 build 2834
Platform	Windows 64 bit

Appendix C. Flight 2B Report

Agisoft PhotoScan Flight 2B

Processing Report
06 March 2017

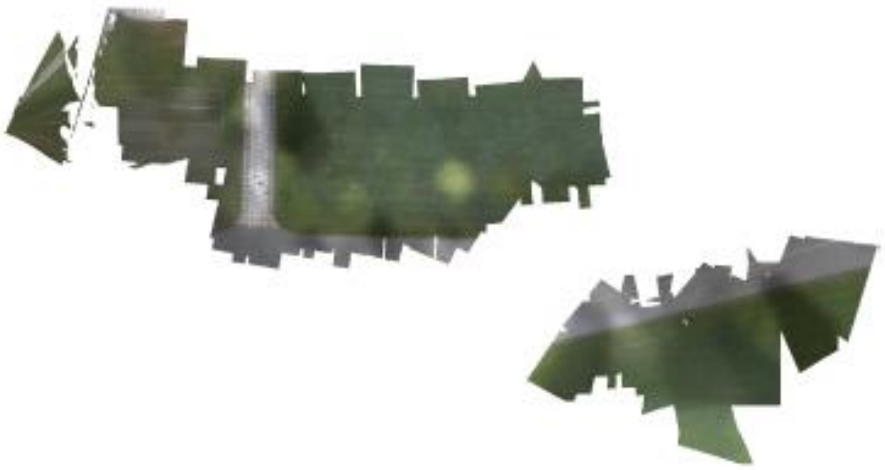

Survey Data

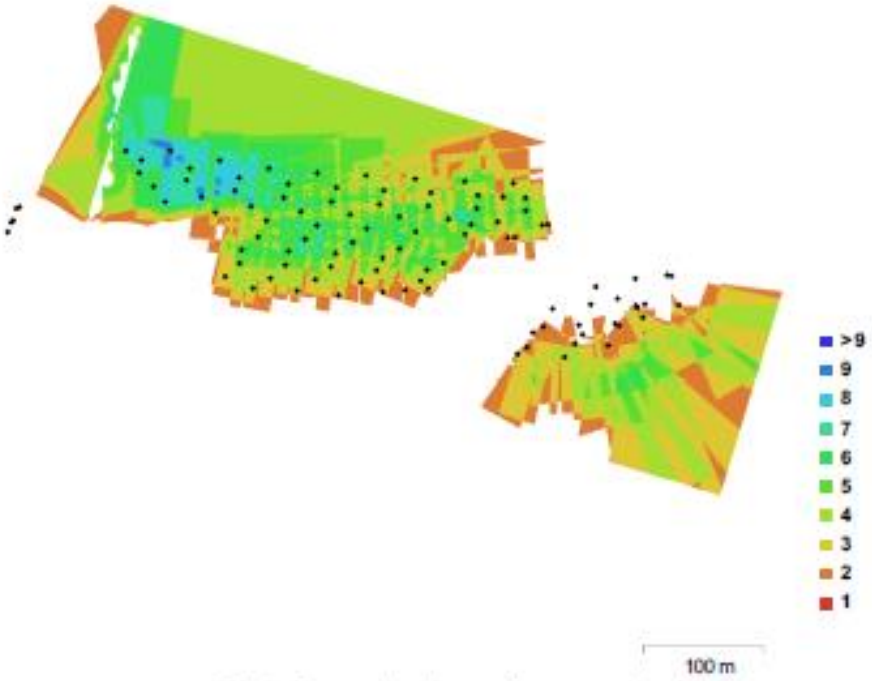

Fig. 1. Camera locations and image overlap.

Number of images:	169	Camera stations:	101
Flying altitude:	63.7 m	Tie points:	212,732
Ground resolution:	1.11 cm/pix	Projections:	498,727
Coverage area:	0.0888 km²	Reprojection error:	0.928 pix

Camera Model	Resolution	Focal Length	Pixel Size	Precalibrated
Canon EOS REBEL SL1 (24 mm)	5184 x 3456	24 mm	4.38 x 4.38 µm	No

Table 1. Cameras.

Camera Calibration

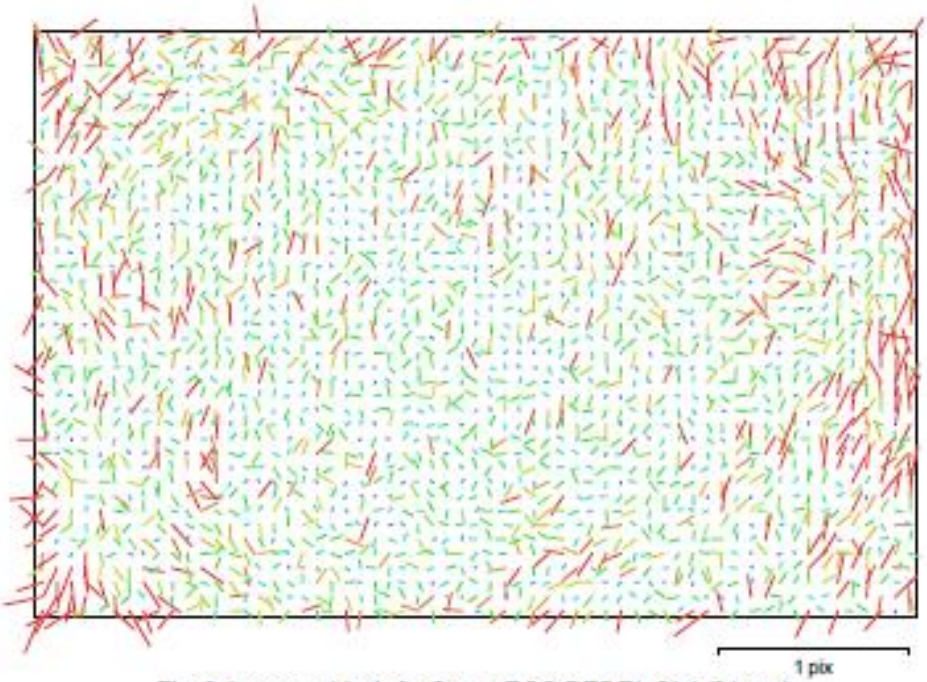

Fig. 2. Image residuals for Canon EOS REBEL SL1 (24 mm).

Canon EOS REBEL SL1 (24 mm)

169 images

Resolution	Focal Length	Pixel Size	Precalibrated
5184 x 3456	**24 mm**	**4.38 x 4.38 µm**	**No**

Type:	Frame	F:	5749.54
Cx:	0	B1:	4.46741
Cy:	0	B2:	3.75277
K1:	-0.128006	P1:	-0.000678035
K2:	0.135107	P2:	0.000681742
K3:	0	P3:	0
K4:	0	P4:	0

Camera Locations

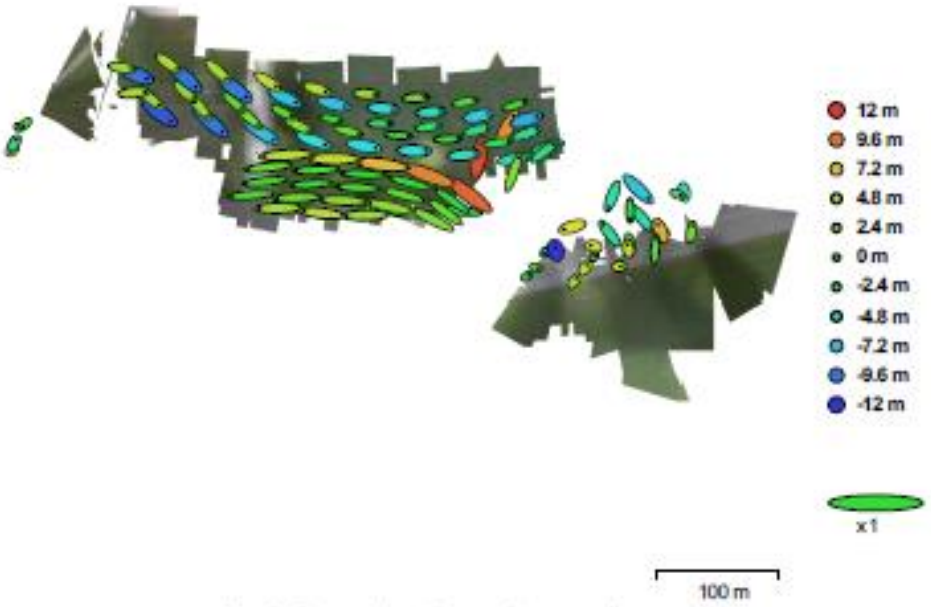

Fig. 3. Camera locations and error estimates.
Z error is represented by ellipse color. X,Y errors are represented by ellipse shape.
Estimated camera locations are marked with a black dot.

X error (m)	Y error (m)	Z error (m)	XY error (m)	Total error (m)
19.059	8.90963	4.78042	21.0387	21.5749

Table 2. Average camera location error.

Digital Elevation Model

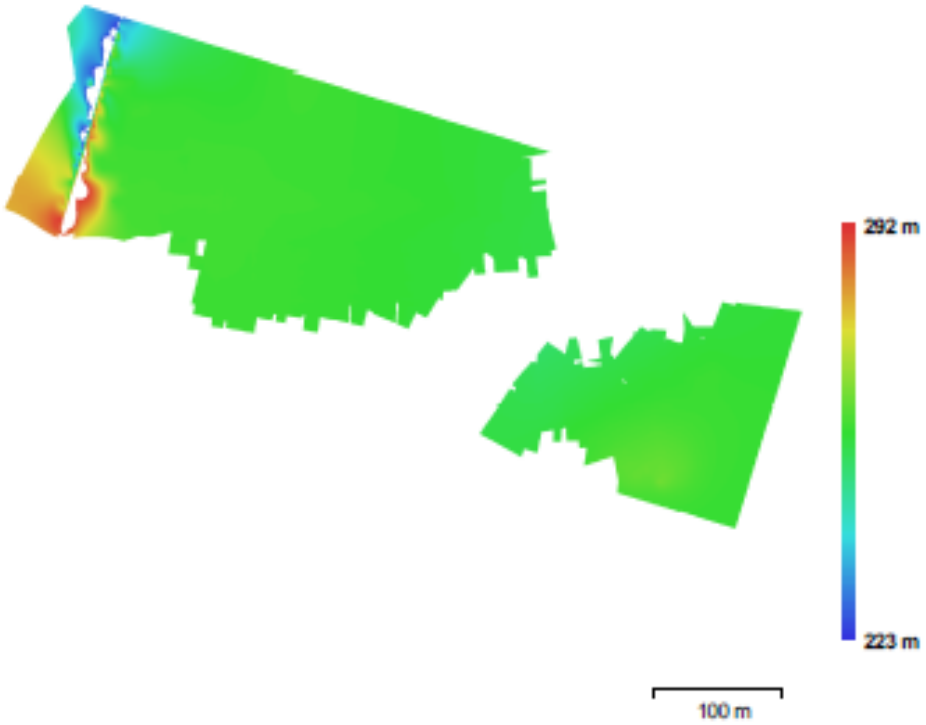

Fig. 4. Reconstructed digital elevation model.

Resolution:	37.8 cm/pix
Point density:	6.99 points/m²

Processing Parameters

General	
Cameras	169
Aligned cameras	101
Coordinate system	WGS 84 (EPSG::4326)
Point Cloud	
Points	212,732 of 328,273
RMS reprojection error	0.1173 (0.928487 pix)
Max reprojection error	0.353293 (16.4269 pix)
Mean key point size	7.91388 pix
Effective overlap	2.37894
Alignment parameters	
Accuracy	High
Pair preselection	Reference
Key point limit	40,000
Tie point limit	10,000
Constrain features by mask	No
Adaptive camera model fitting	Yes
Matching time	10 minutes 18 seconds
Alignment time	1 minutes 52 seconds
DEM	
Size	1,816 x 1,110
Coordinate system	WGS 84 (EPSG::4326)
Reconstruction parameters	
Source data	Sparse cloud
Interpolation	Enabled
Processing time	2 seconds
Orthomosaic	
Size	56,503 x 36,918
Coordinate system	WGS 84 (EPSG::4326)
Channels	3, uint8
Blending mode	Mosaic
Reconstruction parameters	
Surface	DEM
Enable color correction	No
Processing time	5 minutes 13 seconds
Software	
Version	1.2.6 build 2834
Platform	Windows 64 bit

Appendix D. Flight 3B Report

Agisoft PhotoScan Flight 3B

Processing Report
06 March 2017

Survey Data

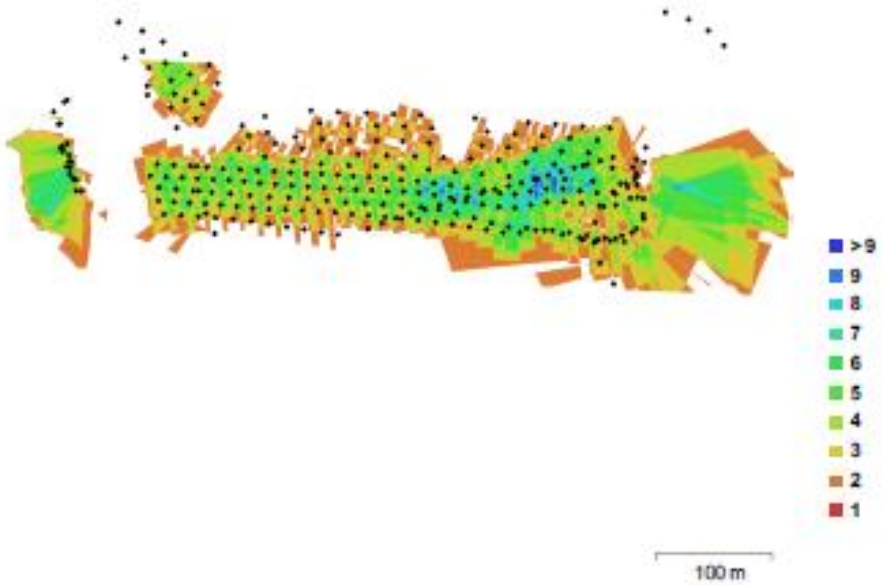

Fig. 1. Camera locations and image overlap.

Number of images:	399	Camera stations:	283
Flying altitude:	37.5 m	Tie points:	727,753
Ground resolution:	6.53 mm/pix	Projections:	1,848,903
Coverage area:	0.0629 km²	Reprojection error:	0.752 pix

Camera Model	Resolution	Focal Length	Pixel Size	Precalibrated
Canon EOS REBEL SL1 (24 mm)	5184 x 3456	24 mm	4.38 x 4.38 µm	No

Table 1. Cameras.

Camera Calibration

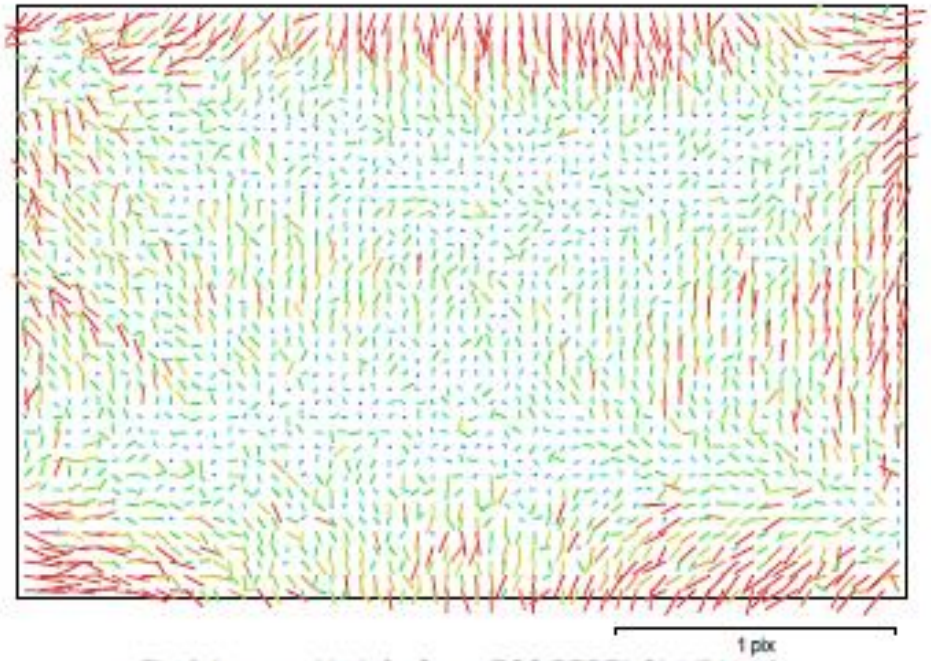

Fig. 2. Image residuals for Canon EOS REBEL SL1 (24 mm).

Canon EOS REBEL SL1 (24 mm)

399 images

Resolution	Focal Length	Pixel Size	Precalibrated
5184 x 3456	**24 mm**	**4.38 x 4.38 µm**	**No**

Type:	Frame	F:	5749.29
Cx:	-31.375	B1:	-11.108
Cy:	40.7268	B2:	7.05783
K1:	-0.132362	P1:	-0.000498245
K2:	0.16003	P2:	0.000669044
K3:	-0.082007	P3:	0
K4:	0.0496304	P4:	0

Camera Locations

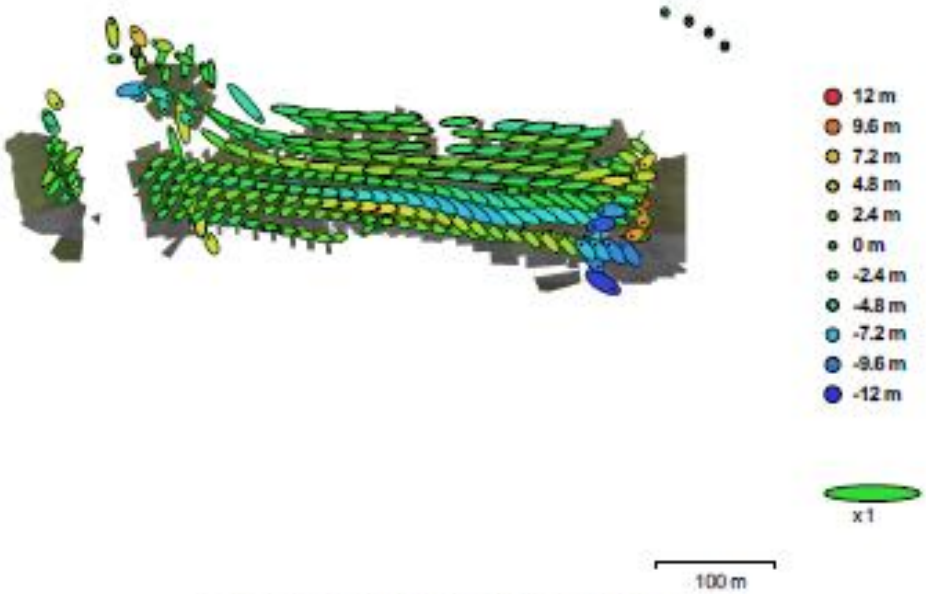

Fig. 3. Camera locations and error estimates.
Z error is represented by ellipse color. X,Y errors are represented by ellipse shape.
Estimated camera locations are marked with a black dot.

X error (m)	Y error (m)	Z error (m)	XY error (m)	Total error (m)
15.9226	7.51157	3.29991	17.6055	17.9121

Table 2. Average camera location error.

Digital Elevation Model

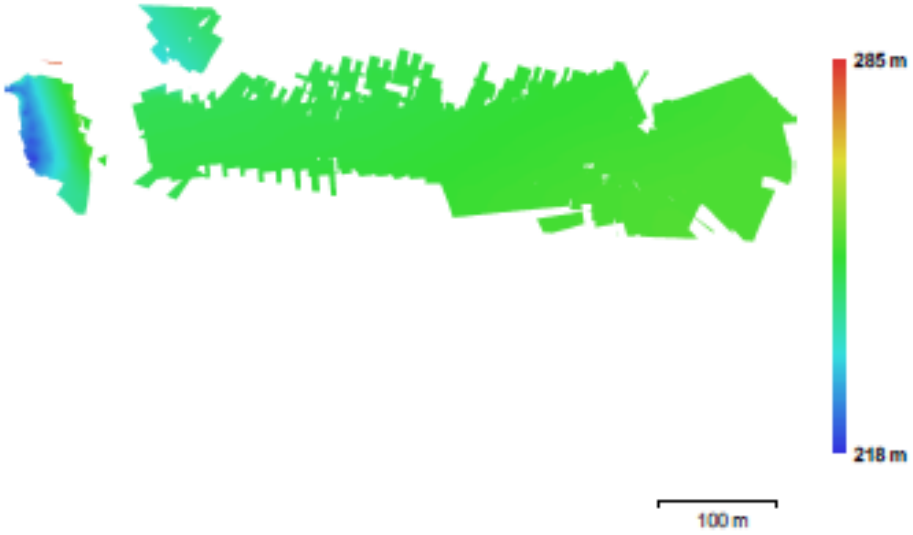

Fig. 4. Reconstructed digital elevation model.

Resolution:	20.6 cm/pix
Point density:	23.6 points/m²

Processing Parameters

General	
Cameras	399
Aligned cameras	283
Coordinate system	WGS 84 (EPSG::4326)
Point Cloud	
Points	727,753 of 939,530
RMS reprojection error	0.13068 (0.751504 pix)
Max reprojection error	0.394128 (21.4753 pix)
Mean key point size	5.45828 pix
Effective overlap	2.54609
Alignment parameters	
Accuracy	High
Pair preselection	Reference
Key point limit	40,000
Tie point limit	10,000
Constrain features by mask	No
Adaptive camera model fitting	Yes
Matching time	25 minutes 19 seconds
Alignment time	6 minutes 59 seconds
DEM	
Size	3,342 x 1,008
Coordinate system	WGS 84 (EPSG::4326)
Reconstruction parameters	
Source data	Sparse cloud
Interpolation	Enabled
Processing time	7 seconds
Orthomosaic	
Size	102,836 x 30,895
Coordinate system	WGS 84 (EPSG::4326)
Channels	3, uint8
Blending mode	Mosaic
Reconstruction parameters	
Surface	DEM
Enable color correction	No
Processing time	12 minutes 52 seconds
Software	
Version	1.2.6 build 2834
Platform	Windows 64 bit

Bibliography

Anderson, M. L., Pasque, P., Lane, C., & Pond, J. (2017). Autonomous System for Rapid Airfield Assessment. *AIAA Information Systems-AIAA Infotech @ Aerospace*, (January), 1–8. http://doi.org/10.2514/6.2017-1158

Ajayi, O. G., Salubi, A. A., Angbas, A. F., & Odigure, M. G. (2017). Generation of accurate digital elevation models from UAV acquired low percentage overlapping images. *International Journal of Remote Sensing*, *0*(0), 1–22. http://doi.org/10.1080/01431161.2017.1285085

Barry, P., & Coakley, R. (2013). Field accuracy test of RPAS photogrammetry. *International Archives of the Photogrammetry, Remote Sensing and Spatial Information Sciences - UAVg2013*, *XL-1/W2*, 27–31.

Canon SL1 Review - Performance. (n.d.). Retrieved February 11, 2017, from http://www.imaging-resource.com/PRODS/canon-sl1/canon-sl1A6.HTM

Clement, M. R., Bourakov, E., Jones, K. D., & Dobrokhodov, V. (2009). *Unmanned Systems Control and Data Dissemination*.

Department of Defense. (2008). *Airfield and Heliport Planning and Design* (UFC 3-260-01). Retrieved from https://www.wbdg.org/FFC/DOD/UFC/ufc_3_260_01_2008.pdf

Endsley, M. (2015). *Autonomous Horizons* (Vol. I). USAF: Office of the Chief Scientist.

Gendreau, H., & Levin, A. (2017). Lady Gaga Halftime Drone Swarm Was Pretaped to Shield Crowd - Bloomberg. Retrieved February 10, 2017, from https://www.bloomberg.com/news/articles/2017-02-07/lady-gaga-s-halftime-drone-swarm-was-pretaped-to-shield-crowd

Grandsaert, P. J. (2015). *Integrating Pavement Crack Detection and Analysis Using Autonomous Unmanned Aerial Vehicle Imagery*. Retrieved from http://www.dtic.mil/docs/citations/ADA615401

Green, T. (2016). United States Air Force Civil Engineers 2016 – 2036 Civil Engineer Flight Plan.

Greenwood, F. (2015). How to make maps with drones. *Drones and Aerial Observation*, (July), 35–47.

Gross, J. W. (2015). A Comparison of Orthomosaic Software for Use with Ultra High Resolution Imagery of a Wetland Environment, 15.

Holman, F. H., Riche, A. B., Michalski, A., Castle, M., Wooster, M. J., & Hawkesford, M. J. (2016). High Throughput Field Phenotyping of Wheat Plant Height and Growth Rate in Field Plot Trials Using UAV Based Remote Sensing. http://doi.org/10.3390/rs8121031

Irizarry, J., Gheisari, M., & Walker, B. N. (2012). Usability assessment of drone technology as safety inspection tools. *Electronic Journal of Information Technology in Construction*, *17*(September), 194–212.

Jensen, J. L. R., & Mathews, A. J. (2016). Assessment of image-based point cloud products to generate a bare earth surface and estimate canopy heights in a woodland ecosystem. *Remote Sensing*, *8*(1). http://doi.org/10.3390/rs8010050

Koh, L. P., & Wich, S. A. (2012). Dawn of drone ecology: low-cost autonomous aerial vehicles for conservation. *Tropical Conservation Science*, *5*(2), 121–132. http://doi.org/WOS:000310846600002

Klette, R. (2014). *Concise Computer Vision - An Introduction into Theory | Reinhard Klette | Springer*. Springer Science and Business Media. Retrieved from http://www.springer.com/us/book/9781447163190

McIntosh, A. (2016). Boeing affiliate Insitu donates ScanEagle unmanned aircraft drone to Smithsonian National Air and Space Museum in Chantilly Virginia - Puget Sound Business Journal. Retrieved February 11, 2017, from http://www.bizjournals.com/seattle/news/2016/12/22/boeing-affiliate-insitu-donates-scaneagle-drone-to.html

Meeks, M. T. (2016). *Evaluating Storm Sewer Pipe Condition Using Autonomous Drone Technology*. Retrieved from http://www.dtic.mil/docs/citations/

Meier, L., Tanskanen, P., Fraundorfer, F., & Pollefeys, M. (2012). the Pixhawk Open-Source Computer Vision Framework for Mavs. *ISPRS - International Archives of the Photogrammetry, Remote Sensing and Spatial Information Sciences*, *XXXVIII-1/*(September), 13–18. http://doi.org/10.5194/isprsarchives-XXXVIII-1-C22-13-2011`

Morgenthal, G., & Hallermann, N. (2014). Quality Assessment of Unmanned Aerial Vehicle (UAV) Based Visual Inspection of Structures. *Advances in Structural Engineering*, *17*(3), 289–302. http://doi.org/10.1260/1369-4332.17.3.289

MTU, M. (2015). Evaluating the Use of Unmanned Aerial Vehicles for Transportation Purposes III, *RC-1616*. Retrieved from http://www.michigan.gov/mdot/0,4616,7-151-9622_11045_24249_52176-353767--,00.html

Nex, F., & Remondino, F. (2014). UAV for 3D mapping applications: A review. *Applied Geomatics*. http://doi.org/10.1007/s12518-013-0120-x

RobotShop. (n.d.). LIDAR-Lite 2 Laser Rangefinder (PulsedLight) - RobotShop. Retrieved January 1, 2016, from http://www.robotshop.com/en/lidar-lite-2-laser-rangefinder-pulsedlight.html

Schnebele, E., Tanyu, B. F., Cervone, G., & Waters, N. (2015). Review of remote sensing methodologies for pavement management and assessment. *European Transport Research Review*, *7*(2). http://doi.org/10.1007/s12544-015-0156-6

Shel-Daat, T. (n.d.). Gnostic Students Network. Retrieved April 9, 2015, from https://plus.google.com/communities/102119423336749494689/stream/7b2e19a2-a91f-40ee-b648-9803550cc9be

Sulebak, J. (2000). Applications of Digital Elevation Models. *DYNAMAP Project Oslo*, 1–11. Retrieved from http://www.gisknowledge.net/topic/terrain_modelling_and_analysis/sulebak_dem_applications_00.pdf

Swain, K. C., Thomson, S. J., & Jayasurya, H. P. W. (2010). Adoption of an unmanned helicopter for low-altitude remote sensing to estimate yield and total biomass of a rice crop. *Transactions of the ASAE …*, *53*(1), 21–27. Retrieved from http://ddr.nal.usda.gov/handle/10113/41029

Szeliski, R. 2010. "Computer Vision: Algorithms and Applications." In , 3: Springer.

Tahar, K., & Ahmad, A. (2013). An Evaluation on Fixed Wing and Multi-Rotor UAV Images using Photogrammetric Image Processing. *International Journal of Computer, Electrical, Automation, Control and Information Engineering*, *7*(1), 48–52. Retrieved from http://www.waset.org/publications

Tatham, P. (2009). An investigation into the suitability of the use of unmanned aerial vehicle systems (UAVS) the initial needs assesment process in rapid onset humanitarian disasters. *International Journal of Risk Assessment and Management*, *13*(1), 60–78. http://doi.org/10.1504/IJRAM.2009.026391

Unmanned Aircraft System Pilot Project | San Diego Gas & Electric. (n.d.). Retrieved February 10, 2017, from http://www.sdge.com/key-initiatives/uas

USAF. (2011). *US Air Force Civil Engineering Strategic Plan*. Retrieved from https://cs1.eis.af.mil/sites/ceportal/SiteCollectionDocuments/2011 U.S. Air Force Civil Engineering Strategic Plan.pdf

Vanier, D. J. "Dana." (2001). Why Industry Needs Asset Management Tools. *Journal of Computing in Civil Engineering*, *15*(1), 35–43. http://doi.org/10.1061/(ASCE)0887-3801(2001)15:1(35)

Wallace, L., Lucieer, A., Malenovsky, Z., Turner, D., & Vopenka, P. (2016). Assessment of forest structure using two UAV techniques: A comparison of airborne laser scanning and structure from motion (SfM) point clouds. *Forests*, *7*(3), 1–16. http://doi.org/10.3390/f7030062

Wildlife Conservation Society. (2014, November 17). Ten ways remote sensing can contribute to conservation. *ScienceDaily*. Retrieved February 9, 2017 from www.sciencedaily.com/releases/2014/11/141117125607.htm

Xiang, H., & Tian, L. (2011). Method for automatic georeferencing aerial remote sensing (RS) images from an unmanned aerial vehicle (UAV) platform. *Biosystems Engineering*, *108*(2), 104–113. http://doi.org/10.1016/j.biosystemseng.2010.11.003

Vita

Mr. Brian Allen graduated from Florida State University in 1998 with a Bachelor of Science in Mechanical Engineering. He spent the next eleven years working as a defense contractor primarily supporting the U.S. Navy. He earned his professional engineer license in 2004.

In 2009 he became the mechanical engineer at Tyndall AFB with project management and development. In 2011, he was assigned as a project programmer at RAF Lakenheath, United Kingdom. In August 2015, he entered the Air Force Institute of Technology at Wright-Patterson AFB, Ohio and earned a Master of Science degree in Engineering Management. Upon graduation, he will be assigned to the Civil Engineer Group at Wright-Patterson AFB.

REPORT DOCUMENTATION PAGE		*Form Approved* *OMB No. 0704–0188*

1. REPORT DATE (DD–MM–YYYY)	2. REPORT TYPE	3. DATES COVERED *(From — To)*
23-03-2017	Master's Thesis	1 Aug 2015 – 23 Mar 2017

4. TITLE AND SUBTITLE	5a. CONTRACT NUMBER
Actionable Stitched Images from an Unmanned Aerial System	5b. GRANT NUMBER
	5c. PROGRAM ELEMENT NUMBER
6. AUTHOR(S) Allen, Brian R., Mr., Civilian	5d. PROJECT NUMBER
	5e. TASK NUMBER
	5f. WORK UNIT NUMBER
7. PERFORMING ORGANIZATION NAME(S) AND ADDRESS(ES) Air Force Institute of Technology Graduate School of 2950 Hobson Way WPAFB OH 45433-7765	8. PERFORMING ORGANIZATION REPORT NUMBER AFIT-ENV-MS-17-M-168
9. SPONSORING / MONITORING AGENCY NAME(S) AND ADDRESS(ES) Mr. Robert Diltz AFCEC 139 Barnes Drive, Suite 2Tyndall AFB, FL, 32403 (937) 255-8769, Robert.Diltz@us.af.mil	10. SPONSOR/MONITOR'S ACRONYM(S)
	11. SPONSOR/MONITOR'S REPORT NUMBER(S)

12. DISTRIBUTION / AVAILABILITY STATEMENT
Distribution Statement A. Approved for Pubic Release, Distribution Unlimited

13. SUPPLEMENTARY NOTES

14. ABSTRACT
This thesis investigates the capability of a commercial off the shelf (COTS) unmanned aerial vehicle, camera, and software to accurately capture and represent a portion of an airfield for condition evaluation. Three separate flight tests were performed exploring different means of camera shutter control and altitudes. The individual images captured were then stitched into a single orthomosaic which provides an aerial view allowing for dimensional measurements and relative location.
The results found show that COTS hardware and software is possible of capturing images with ground resolution of less than 6 mm. The orthomosaic generated was proven to maintain dimensional accuracy. The digital elevation model generated was able to identify terrain elevation differences of less than one foot. This provides a proof of concept that for less than five thousand dollars a civil engineer squadron could have an organic ability to accurately assess and quantify an airfield digitally. This will help ensure the limited resources available get to the right place at the right time.

15. SUBJECT TERMS
Unmanned Aerial System, orthomosaic, pavement condition

16. SECURITY CLASSIFICATION OF:			17. LIMITATION OF ABSTRACT	18. NUMBER OF PAGES	19a. NAME OF RESPONSIBLE PERSON
a. REPORT U	b. ABSTRACT U	c. THIS PAGE U	UU	110	John Colombi, PhD (ENV)
					19b. TELEPHONE NUMBER (Include Area Code) (937) 255-3636 x3347 john.colombi@afit.edu

Standard Form 298 (Rev. 8–98)
Prescribed by ANSI Std. Z39.18